

POLITECNICO DI MILANO
School of Industrial and Information Engineering
Mechanical Department
Master's degree in Mechanical Engineering



POLITECNICO
MILANO 1863

An integrated numerical test rig for wind tunnel experiments on floating offshore wind turbines

Supervisor: Prof. Hermes GIBERTI
Assistant Supervisor: Ing. Ilmas Andrea BAYATI

Candidate:
Mattia TABAI, matr. 837795

Accademic Year 2016 - 2017

Abstract

The aim of this thesis work deals with the development of a numerical model in Adams/AdWiMo/Simulink environment able to reproduce the experimental tests on floating offshore wind turbines made in the wind tunnel.

The thesis was carried out under the European Community funded LIFES50+ projects, whose purpose is the study and the development of offshore wind turbine systems (10 MW) to be installed in water depths higher than 50 meters.

The numerical model developed in Adams/AdWiMo environment is composed of a scaled wind turbine, with a length scaling factor of $1/75$, and an hexapod robot for the handling of the system, designed and realized by Politecnico di Milano.

A set of static and unsteady (imposed sinusoidal motion) simulations has been carried out in order to validate the numerical model, comparing the results, in terms of Thrust force, both with the data obtained from another simulation environment, FAST, and with the ones obtained in the wind tunnel.

In the second part, the model has been exported in Simulink environment in order to perform a co-simulation for testing it through a hydrodynamical simplified system (2 degrees of freedom, the surge and the pitch). All the issues were analyzed in detail, both the ones related to the torque control of the turbine rotor and the ones related to the effective measurement of the aerodynamic force. The latter must be calculated purifying the inertial and gravitational contribution due to the scaled model, which has different mass and inertia parameters than the reference one.

Numerous simulations were carried out with the numerical model obtained (decay tests at different wind conditions, regular and irregular sea states with and without wind) in order to validate the final system, comparing the results with the experimental tests realized in the wind tunnel and in the ocean basin.

Sommario

Lo scopo del seguente lavoro di tesi consiste nello sviluppare un modello numerico in ambiente Adams/AdWiMo/Simulink capace di riprodurre le prove sperimentali, effettuate in galleria del vento, atte a testare una turbina eolica galleggiante.

La tesi è stata svolta nell'ambito del progetto LIFES50+, finanziato dall'Unione Europea, il cui scopo è lo studio e lo sviluppo di sistemi eolici (10 MW) offshore galleggianti, da installare in acque profonde (più di 50 m di profondità).

Il modello numerico sviluppato in ambiente Adams/AdWiMo è composto da una turbina eolica scalata, con fattore di scalatura 1/75, e da un robot esapode per la movimentazione del sistema, progettato e realizzato da Politecnico di Milano.

Sono state effettuate quindi prove statiche e a moto imposto atte a validare il modello numerico, confrontando i risultati ottenuti, in termini di forza di Thrust, sia con i dati ottenuti da un altro ambiente simulativo, FAST, sia con quelli ottenuti in galleria del vento.

Si è poi passati a una co-simulazione in ambiente Simulink, dove si è testato il sistema attraverso un modello idrodinamico semplificato (2 gradi di libertà, surge e pitch). Sono state analizzate nel dettaglio tutte le problematiche dovute sia al controllo in coppia del rotore della turbina sia all'effettiva misurazione della forza aerodinamica. Quest'ultima deve essere calcolata depurando il contributo inerziale e gravitazione dovuto al modello scalato, che presenta parametri di massa e inerzia differenti rispetto a quello di riferimento.

Con il modello numerico ottenuto è stata condotta una serie di simulazioni (decay test a diverse condizioni di vento, forzante ondosa regolare e irregolare con e senza vento) in modo da validare il sistema finale, confrontando i risultati con le prove sperimentali effettuate in galleria del vento e in vasca navale.

Ringraziamenti

Durante questi 12 mesi, nei quali ho svolto il mio lavoro di tesi, ho collaborato e conosciuto diverse persone, ognuna delle quali ha arricchito il mio percorso di studi e per questo devo a loro un ringraziamento.

Il mio primo ringraziamento è per il Prof. Hermes Giberti, per i suoi numerosi insegnamenti e per avermi permesso di lavorare a questo stimolante progetto.

Un dovuto e sincero grazie va agli ingegneri Ilmas Andrea Bayati, Luca Bernini e Enrico Fiore, per tutti i consigli e gli aiuti ricevuti in questo anno di lavoro insieme, ma soprattutto per avermi sempre fatto sentire parte attiva del gruppo.

Ringrazio i miei coinquilini Alberto, Daniele, Pietro e Tommaso, per tutti gli anni passati assieme, sicuro che l'amicizia creatasi continuerà anche dopo questa esperienza.

Ai miei amici, che mi hanno accompagnato per tutti questi anni e che sono stati una valvola di sfogo fondamentale nei periodi più intensi.

A Martina, che mi ha supportato in questi ultimi anni, dandomi la forza per proseguire al meglio questo mio percorso.

Infine, a Giancarlo, Cristina e Elia, che mi hanno permesso tutto questo, un semplice grazie non basterebbe.

Contents

Abstract	i
Sommario	iii
1 Introduction	1
1.1 Wind Energy	1
1.2 Offshore Wind Turbines	3
1.3 AdWiMo	6
1.4 FAST	7
2 State of art	9
2.1 LIFES50+ Project	9
2.2 LIFES50+ Project at Politecnico di Milano	11
2.2.1 Scaled model turbine	11
2.2.2 Wind tunnel tests and AeroDyn validation	13
2.2.3 Robotic Platform	17
2.2.4 Main activities of the thesis	19
3 Modeling	21
3.1 AdWiMo environment	21
3.2 Scaled Wind Turbine	24
3.2.1 Tower	24
3.2.2 Blades	26
3.2.3 Hub, Mainshaft, Mainframe and Generatorframe	33
3.2.4 Creation of the turbine	33
3.2.5 Aerodynamic forces	36
3.2.6 Rotor control	36
3.3 Robot	38
3.4 Co-simulation in Simulink environment	42

4	Validation of the model	45
4.1	Modal analysis	46
4.2	Steady analysis	52
4.3	Unsteady analysis	56
5	Hydrodynamic model	63
5.1	Hydrodynamic Numerical Model	64
5.1.1	Time domain numerical model	67
5.2	Experimental setup and implementation	70
5.2.1	Real model	71
5.2.2	Control and actuation model	73
5.3	AdWiMo-Simulink HIL model	76
5.4	Wind tunnel tests	80
5.4.1	Decay tests	80
5.4.2	Regular wave tests	84
5.4.3	Irregular wave tests	86
6	Conclusions and future developments	89
A	Creation of the model in AdWiMo environment	91
B	Implementation issues	99
C	Input file for the tower	103
D	Input file for the blades	105
E	Output file for the aerodynamic forces calculated by Aero-Dyn	115

List of Figures

1.1	Prof. James Blyth's windmill	1
1.2	Gansu Wind Farm	2
1.3	Worldwide electricity generation from wind from 1989 to 2012	3
1.4	Offshore wind farm	4
1.5	Fixed offshore foundations: Monopile - Tripod - Jacket - Suction Caisson - Gravity base	5
1.6	Floating offshore foundations: Spar Buoy - Tension Leg Platform - Barge	6
2.1	The four substructures to be studied	10
2.2	Wind tunnel test setup	14
2.3	Performances for velocity scale factor 3 as function of wind speed	15
2.4	Unsteady results over static curve	15
2.5	6-Dof Robotic Platform "HexaFloat"	17
2.6	"Hexaslide" robot modeled in Adams	18
2.7	Adams/AdWiMo numerical model scheme	19
3.1	Adwimo input and data flow [13]	22
3.2	Geometry of tower [13]	25
3.3	Blade and CRS reference frames [13]	27
3.4	Interpolation nodes for chord, twist and relative thickness of the blades	31
3.5	Comparison between real and AdWiMo scaled blade	32
3.6	Layout of the nacelle zone [9]	33
3.7	Scaled wind turbine in Adwimo environment	35
3.8	Rotor control logic	37
3.9	CAD model of the platform	39
3.10	Turbine-robot system in Adwimo environment	41
3.11	Simulink model of the AdWiMo system	44

4.1	First mode of vibration of the tower	49
4.2	Second mode of vibration of the tower	49
4.3	First flap-wise mode of vibration of the blade	50
4.4	Second flap-wise mode of vibration of the blade	50
4.5	Polimi wind turbine modes of vibration	52
4.6	Performances of DTU 10 MW scaled wind turbine	54
4.7	Thrust results for steady analysis on Polimi turbine compared to the target curves	56
4.8	Flowchart for the data process leading the detection of the aerodynamic force only from the imposed motion tests [7] . .	59
4.9	Thrust analysis for unsteady tests: comparison between nu- merical results (AdWiMo and FAST) and experimental ones .	60
4.10	Torque analysis for unsteady tests: comparison between nu- merical results (AdWiMo and FAST) and experimental ones .	60
4.11	Hysteresis cycles obtained from the unsteady tests: compari- son between experimental and numerical results	61
5.1	Regular waves	65
5.2	Validity of the different wave theories	66
5.3	Scheme of the complete system	68
5.4	Real model used for wind tunnel tests	71
5.5	2 Dof platform kinematic	72
5.6	Polimi wind turbine rotor and nacelle	73
5.7	Wind tunnel control logic	73
5.8	Forces acting on the physical system	75
5.9	AdWiMo-Simulink HIL control logic	77
5.10	Surge decay tests for different wind conditions	81
5.11	Pitch decay tests for different wind conditions	82
5.12	Fourier transform of the two degrees of freedom for the decay test	83
5.13	Regular wave test in no wind condition	85
5.14	Regular wave test in rated wind condition	85
5.15	Surge result for the irregular wave test in no wind condition .	87
5.16	Pitch result for the irregular wave test in no wind condition .	87
5.17	Surge result for the irregular wave test in rated wind condition	88
5.18	Pitch result for the irregular wave test in rated wind condition	88
A.1	"Create new Database" window	92
A.2	"Macro Read" window	93
A.3	Pre-process commands	94

A.4	"Create a new turbine" window	94
A.5	Aerodynamic forces window	95
A.6	Definition of the imposed rotor motion	96
A.7	"Generator Controller" window	96
A.8	"Adams Control" window	98
B.1	Error on mass properties	102

List of Tables

2.1	Overall parameters of the DTU 10MW Reference Wind Turbine	10
2.2	Scaling factors	12
2.3	FAST/AeroDyn simulation settings	16
3.1	List of the bodies created in Adwimo	23
3.2	Scaling factors used for creating the AdWiMo turbine	24
3.3	Parameters of the tower input file	25
3.4	Scaled tower properties	27
3.5	Blade geometry data block [13]	28
3.6	Blade mass data block [13]	29
3.7	Blade stiffness data block [13]	29
3.8	Blade axis data block [13]	30
3.9	Scaled blade properties	32
3.10	Scaled turbine properties	35
3.11	Inertial parameters of "Hexaslide" robot	40
3.12	Inputs and outputs of the Simulink block	43
4.1	Comparison of the modes of vibration of the DTU 10 MW scaled wind turbine	47
4.2	Real structural parameters of Polimi turbine tower	48
4.3	Comparison of natural frequencies of Polimi turbine	51
4.4	Wind conditions utilized for steady tests	54
4.5	Settings of the different simulations made for the unsteady analysis	58
5.1	Proper frequencies of the two degrees of freedom	84
5.2	Damping parameters for the two degrees of freedom	84
B.1	Issues encountered during the creation of the numerical model	101

Chapter 1

Introduction

1.1 Wind Energy

Wind energy, today, is the use of air flow through wind turbines to mechanically power generators for electric power. Instead, in the past century, it was used to grind grain and pump water.

With the development of electric energy, the wind has been exploited more and more for the production of power. The first windmill used for the production of electric power was built in Scotland in the 1887 by Prof James Blyth of Anderson's College and it was able to lighting some buildings..

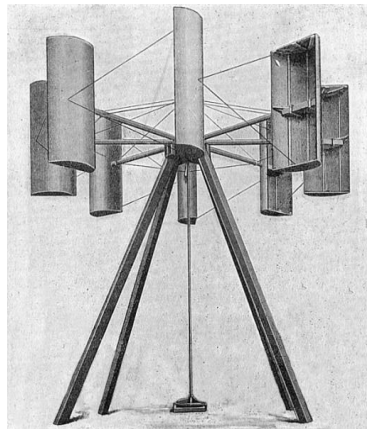


Figure 1.1: Prof. James Blyth's windmill

Throughout the 20th century parallel paths developed small wind stations suitable for farms or residences, and larger utility-scale wind generators that could be connected to electric power grids for remote use of power. Today wind powered generators operate in every size range between tiny stations for battery charging at isolated residences, up to near-gigawatt sized offshore wind farms that provide electric power to national electrical networks.

A large wind farm may consist of several hundred individual wind turbines distributed over an extended area, both onshore and offshore. The largest wind farm in the world is located in Gansu (China) and it is expected to grow to 20,000 MW by 2020, at an estimated cost of 17.5 billion of dollar.



Figure 1.2: Gansu Wind Farm

The success of wind energy is due to the fact that it is a free and renewable source of clean and non-polluting electricity, followed by the development of the technologies needed for an economic and efficient production of turbines.

Despite this, the technology still requires a higher initial investment than fossil energy plant, but, if they are compared in terms of "life-cycle" cost, wind costs are much more competitive because there is no fuel to purchase and minimal operating expenses.

Although wind power plants have relatively little impact on the environment, there is some concern over the noise produced by the rotor blades, visual impacts, and birds having been killed by flying into the rotors. Most

of these problems have been resolved or greatly reduced through technological development or by properly siting wind plants.

Worldwide there are now over two hundred thousand wind turbines operating, with a total nameplate capacity of 432 GW as of end 2015. Wind generation capacity more than quadrupled between 2000 and 2006, doubling about every three years, and the energy production was around 4% of total worldwide electric power usage, and growing rapidly.

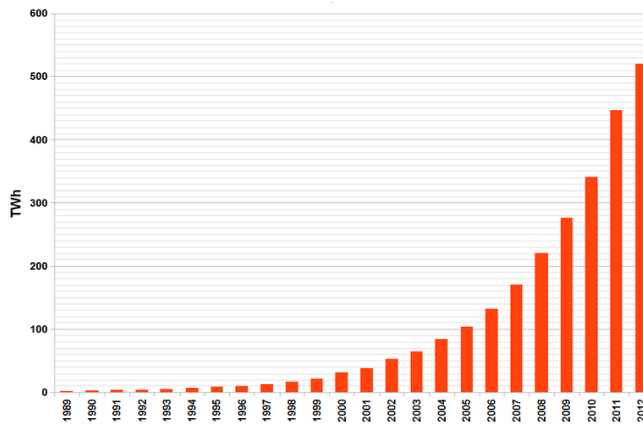


Figure 1.3: Worldwide electricity generation from wind from 1989 to 2012

Europe accounted for 48% of the world total wind power generation capacity in 2009. In 2010, Spain became Europe's leading producer of wind energy, achieving 42,976 GWh. Germany held the top spot in Europe in terms of installed capacity, with a total of 27,215 MW as of 31 December 2010. In 2015 wind power constituted 15.6% of all installed power generation capacity in the EU and it generates around 11.4% of its power.

1.2 Offshore Wind Turbines

Offshore wind power refers to the construction of wind farms in large bodies of water to generate electric power. Unlike the typical usage of the term "offshore" in the marine industry, offshore wind power includes inshore water areas such as lakes, fjords and sheltered coastal areas, utilizing traditional fixed-bottom wind turbine technologies, as well as deeper-water areas uti-

lizing floating wind turbines.



Figure 1.4: Offshore wind farm

These installations can utilize the more frequent and powerful winds that are available in these locations, especially in the afternoon, matching the time when people are using the most electricity. Higher wind speeds do not automatically result in increased electricity generation. Wind turbines are limited by the maximum wind speeds their mechanical and electrical components can reliably and durably operate at. Wind speeds above those limits result in the wind turbine adjusting its blade angles to reduce generator speed or in some cases shutting down entirely. Sustained high-speed operation and generation increases wear, maintenance and repair costs. Furthermore they have less aesthetic impact on the landscape than land based projects allowing bigger dimension of the rotor diameter.

On the contrary, the costs related to offshore turbines are greater than the onshore ones, the US Energy Information Agency said "offshore wind power is the most expensive energy generating technology being considered for large scale deployment", the prices could be in the range of 2.5-3.0 million Euro/MW.

Locating wind turbines offshore exposes the units to high humidity and salt water which negatively affect service life, cause corrosion and oxidation, increase maintenance and repair costs and in general make every aspect of installation and operation much more difficult, time-consuming, more dangerous and far more expensive than sites on land. The humidity and tem-

perature is controlled by air conditioning the sealed nacelle. Research and development projects aim to increase the efficiency and to reduce costs related to offshore wind energy in order to make it competitive respect to the onshore one.

The offshore wind turbines can be divided into two groups according to the depth of the zone in which they are installed, and consequently to the type of their foundation: fixed or floating ones.

The foundations are designed in function of the geotechnical characteristics of the place (depth and sedimentary nature of the backdrop) and the wind and waves conditions.

The first and the most tested ones are the monopile and gravity base foundations, but the increase, in the last years, of projects in deeper water has justify the development of floating structures.

The fixed foundation turbines are principally installed in shallow waters (approximately 20 meters) with a single pylon to the backdrop or under the weight action of concrete foundations, depending on the nature of the land.

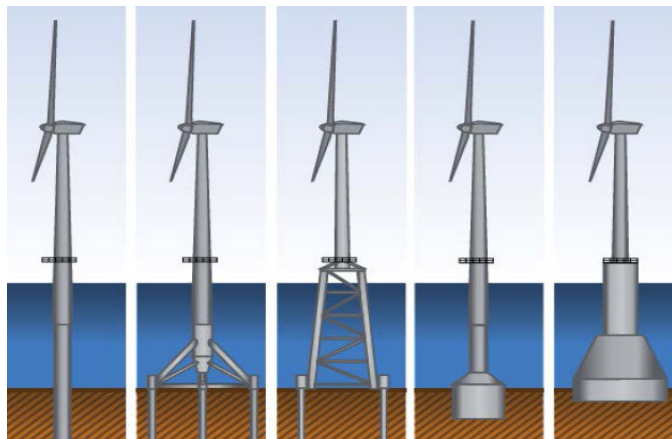


Figure 1.5: Fixed offshore foundations: Monopile - Tripod - Jacket - Suction Caisson - Gravity base

The floating foundation turbines are born from different needs: decrease the environmental impact of the fixed ones, offer the possibility to move the system but primarily the opportunity to install the turbine in higher depths. According to the floating system, three main different types can be classified: a deep balanced buoy that can be anchored through chains or pulled

ropes ("spar buoy"), a tension leg platform (TLP) and a barge at sea level.

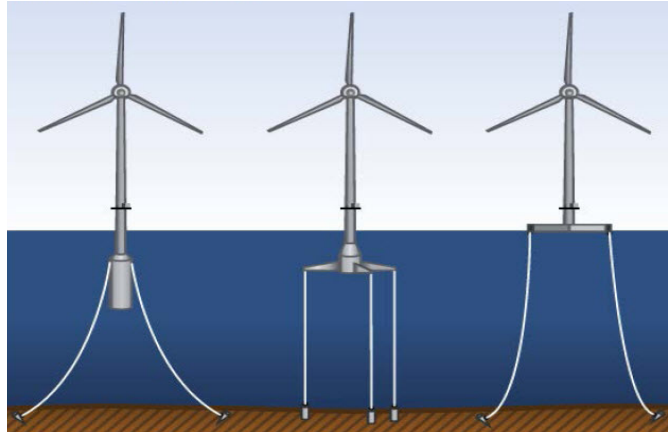


Figure 1.6: Floating offshore foundations: Spar Buoy - Tension Leg Platform - Barge

1.3 AdWiMo

AdWiMo, an acronym for Advanced Wind Turbine Modeling, is an Adams plug-in, developed by MSC.Software, with all the necessary features to assemble a complete and parametric wind turbine and to simulate single or multiple wind fields.

AdWiMo considers every major aspect of turbine design including tower, blades, hub, mainframe, gearbox housing, bearings, transmission, controls (generator, pitch, yaw), aerodynamic and centrifugal forces, Coriolis acceleration, gyroscopic moments, point loads, gravity, thermal loads, and wave loads.

The tool offers a user-friendly and scalable solution for the complete design process of a wind turbine. A simplified wind turbine from the conceptual design phase can be expanded with more complex subsystems such as gears and rolling bearings and/or by replacing rigid bodies with flexible bodies.

The tower and the blades can be modeled as flexible bodies, to take into account the geometric non-linearity present for long parts, through the NASTRAN pre-processors *tower_by_beam* and *blade_by_beam*.

The aerodynamic forces are calculated using the external subroutine *aerodyn13* developed by NREL (National Renewable Energy Laboratory).

For this master thesis, AdWiMo was chosen as the reference numerical tool due to the fact that it allows, besides the creation of the wind turbine, the possibility of interfacing with other programs like Adams and Matlab Simulink, giving the opportunity to have an unique model that considers all the points of interest of the work.

The main difficulty encountered using AdWiMo has been the creation of a scaled wind turbine, the one needed for wind tunnel test. The software has been created for perfectly simulate full scale turbines (its reference model is the 5MW NREL wind turbine) while it encounters problems when the user tries to model a scaled machine, in particular it is not able to properly calculate mass and inertia of some bodies located in the nacelle zone. A specific macro that overcomes this difficulty has been provided by MSC.Software.

1.4 FAST

FAST, an acronym for *Fatigue, Aerodynamics, Structures and Turbulence*, is a comprehensive aeroelastic simulator capable of predicting both the extreme and fatigue loads of two or three bladed horizontal axis wind turbines [9].

The areodynamic component is calculated in the time domain *AeroDyn* module. It calculates the aerodynamic loads, on both blades and tower, based on the principles of actuator lines, where the three dimensional flow around a body is approximated by local two dimensional flow at cross sections. The distributed pressure and shear stresses are supposed equal to lift and drag forces plus pitching moments lumped at a node [10].

The analysis nodes are distributed along the length of each blade and tower, the 2D forces and moments at each node are computed as distributed loads per unit length, and the total 3D aerodynamic loads are founded by integrating them. The discretization of areodynamic analysis may be different from the structural modules one.

The actuator line approximations restrict the validity of the model to slender structures and 3D behaviour is either neglected, captured through corrections inherent in the model or in the input data.

The blade airfoil aerodynamic can be steady or unsteady. In the steady model, the static airfoil data are used directly to calculate nodal loads, while the unsteady one accounts for flow hysteresis, including unsteady attached flow, trailing-edge flow separation, dynamic stall and flow reattachment.

FAST includes the possibility to develop periodic state matrices for controls design and to use itself as a preprocessor for generating ADAMS dataset of wind turbine models. Furthermore AdWiMo uses the same module of FAST to calculate the aerodynamic loads through the subroutine *aerodyn13*, giving the opportunity to exploit the results previously obtained with FAST to validate the AdWiMo model.

Chapter 2

State of art

2.1 LIFES50+ Project

The European Horizon2020-funded program LIFES50+, led by Norway's MARINTEK and involving Politecnico di Milano, is a three years project that will focus on proving the innovative technology that is being developed for floating substructures for 10MW wind turbines at water depths greater than 50m [11].

The program involves twelve different partners, both from university and industry, that are trying to identify the most effective way of reducing the costs related to offshore wind farms of large wind turbines.

The approach consists in finding, starting from four different types of already studied 5 MW offshore wind turbines that have to be upscaled to 10 MW, the two better configurations, in terms of performances and costs, from an experimental and numerical investigation. The target is a Technology Readiness Level (TRL) of 5.

Ultimately, the project will facilitate innovation and competition in the industry, reduce risks, and therefore contribute to a lower levelized cost of energy.

Regarding the wind turbine, the 3 blades 10 MW DTU (Denmark Technical University) has been chosen as reference and it has been implemented in FAST, in order to have a validation of the software and to serve as a reference for floating substructure design and for optimisation of the following activities carried out during the project.

A systematic assessment of the FAST model implementation was carried out, starting with verifying isolated component of the natural frequencies

as well as whole system natural frequencies. The steady state performance of the FAST model implementation was compared against HAWC2 (the numerical software used by DTU), with good overall agreement [12].



Figure 2.1: The four substructures to be studied

Cut in wind speed [m/s]	4
Cut out wind speed [m/s]	25
Rated wind speed [m/s]	11.4
Rated power [MW]	10
Rotor diameter [m]	178.3
Hub height [m]	119.0
Minimum rotor speed [rpm]	6.0
Maximum rotor speed [rpm]	9.6
Rotor Mass [Kg]	227962
Tower Mass [Kg]	628442

Table 2.1: Overall parameters of the DTU 10MW Reference Wind Turbine

2.2 LIFES50+ Project at Politecnico di Milano

Politecnico di Milano Wind Tunnel constitutes a useful and powerful tool to test the aerodynamics of the wind turbines. A proper scaled model is necessary to perform correct analysis that can be compared to the real-scale turbine.

2.2.1 Scaled model turbine

The scaling procedure is based on the application of classical similarity rules. Two coefficients, one related to length and one related to speed, are needed to obtain all the parameters connected to the scaled model, both in terms of structural and mass dimensions and both in terms of wind and external conditions.

The scale factor has been selected considering the following constraints [8]:

- the wind tunnel boundary layer test section dimensions set a physical limit to the length scale factor λ_L , this must be as large as possible, but it must ensure an acceptable solid blockage level and a correct reproduction of the natural gradient;
- the highest possible scale factor for the velocities λ_V to reduce the Reynolds number difference between full scale and model scale and to have high wind speed while testing to optimise the noise to signal ratio of the acquired signals;
- the TSR (tip speed ratio) equals at full scale and at model scale, implying a very high main shaft angular velocity and a very high bandwidth for the IPC (Blade Individual Pitch Control) controllers.

The scale factor is defined as the ratio between a general DTU 10 MW turbine parameter and the corresponding PoliMi 10MW WTM (wind tunnel model) parameter. The length factor has been defined as the ratio between the rotor diameters and it is equal to 75, while the velocities factor could be equal to 2 or 3 because the rotor is designed to work at PoliMi wind tunnel wind speed range. Starting from this two coefficients it is possible to obtain all the ones related to the other physical quantities, like shown in the table 2.2.

A different solution has been considered about the aerodynamic characteristics of the scaled model. It was not possible to use the same blade

profiles of the full-scale 10 MW turbine and scale them using the two obtained coefficients, due to the impossibility of matching the Reynolds number with respect to the real case [6].

Length	[m]	λ_L
Speed	[m s ⁻¹]	λ_V
Ω	[rad s ⁻¹]	λ_V/λ_L
Frequency	[s ⁻¹]	λ_V/λ_L
Acceleration	[m s ⁻²]	λ_V^2/λ_L
Mass	[Kg]	λ_L^3
Inertia	[Kg m ²]	λ_L^5
Force	[N]	λ_V^2/λ_L^2
Torque	[N m]	λ_V^2/λ_L^3
Reynolds	[-]	λ_V/λ_L

Table 2.2: Scaling factors

The goals of the blade design were:

- matching the reference thrust coefficient;
- matching the first blade flap-wise natural frequency;
- matching the scaled blade weight.

The main target for model design is the thrust force, the objective was to match with the lowest possible error the thrust obtained scaling the real one of the 10 MW turbine. The most important parameter is then the lift coefficient C_l .

As said previously, the Reynolds number is different from the full-scale one, approximately 150 times lower with the chosen scaling coefficients. It is evident that the flow regime in full-scale condition is different with respect to the model, which is also consistent with the choice of a different airfoil for the model. The Reynolds number can be computed as:

$$Re = \frac{\rho \cdot V_{rel}(r) \cdot c(r)}{\mu} \quad (2.1)$$

where $V_{rel}(r)$ is the relative wind speed seen by the blade station r , $c(r)$ the blade section chord and ρ , μ the density and the dynamic viscosity of air in the reference atmospheric conditions.

From equation 2.1 the chord of the blade can be obtained, choosing the SD7032 airfoil profile.

The selected blade was validated through a series of wind tunnel tests in which the lift coefficient C_l , the drag coefficient C_d and the moment coefficient C_m were measured at different Reynolds conditions. The blade chord and twist are obtained coming from the comparison between the model-scale and full-scale lift coefficient curve.

Finally the blade cross section relative thickness have to be defined. The target was to have a very stiff blade compared to the real one because the future tests are intended to be done using a rigid wind turbine model. The design was made considering the SD7032 profile and imposing very high frequencies near the blade root, estimating them with a FEM analysis.

2.2.2 Wind tunnel tests and AeroDyn validation

The scaled model has been tested in the wind tunnel at Politecnico di Milano in order to characterise its performances under steady and unsteady (imposed sinusoidal motion) conditions. The experimental results have been compared to the reference 10 MW wind turbine and then used to validate the numerical tool Aerodyn developed by NREL [7].

The test setup, figure 2.2, consists in a two degrees of freedom mechanical system, the scaled wind turbine is mounted on the mechanism by a 6 components load cell to measure the forces at the base of the tower. Another smaller 6 components load cell is mounted between the nacelle and the tower. The surge (displacement along the x-axis, the same direction of the wind) imposed motion at the tower base is made by two hydraulic actuators pushing a slider, while the pitch (rotation respect the y-axis) is made by a slider-crank mechanism transforming the linear displacement to a rotation. During the tests, a new experimental approach has been implemented in order to overcome the scaling issues associated to the simultaneously loads coming from wind and waves. This approach is called "Hardware in the Loop", the system is subjected to both experimentally measured and numerically computed forces in real time. A more in deep explanation of this method will be carried out in Chapter 5.

The first tests carried out were the steady ones for the investigation of

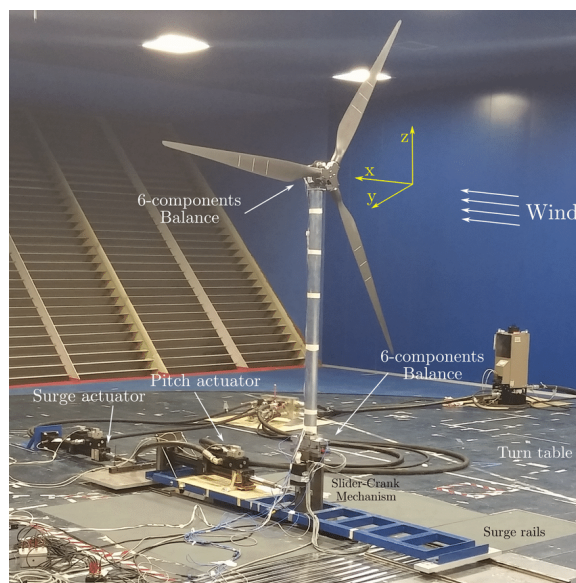


Figure 2.2: Wind tunnel test setup

the turbine performances, that are the thrust and the torque. They show generally a good agreement with the characteristic curves of the DTU 10 MW turbine. The thrust force perfectly matches the real one due to the fact that the blades were design with this target, but a good agreement is also visible for the torque with a greater satisfaction for λ_V equals to 2 up to wind rated condition. With regard to the above rated condition, the discrepancy from the nominal curve can be explained considering the pitch angle of the blades, in fact, for wind speed higher than the rated one, they has been set equal to the values of the DTU designed for different airfoil and flow condition.

Also for the velocities factor equal to 3, good results have been obtained (figure 2.3).

The unsteady tests aim was to show the dependency of imposed amplitude and frequency, for both low and wave frequency range, at each wind turbine working condition (below rated, rated and above rated). They were carried out using $\lambda_V = 3$, it is preferable because of the lower frequencies of the surge and the pitch imposed motion.

The tests consisted in measuring the forces acting on the system under the

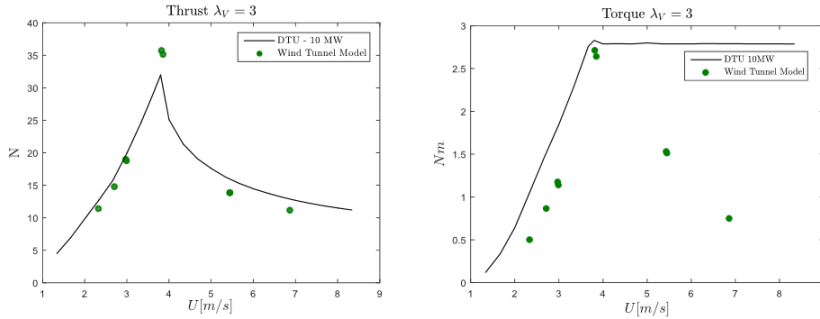


Figure 2.3: Performances for velocity scale factor 3 as function of wind speed

action of the imposed motion and the constant wind. The inertial contribution is significant and it has to be eliminated repeating twice the test with and without the wind. The pure aerodynamic loads have been obtained subtracting the inertial component to the total one paying attention to the possible phase lag introduced by the presence of different measuring tools. The force mainly investigated was the thrust. The results show an hysteretic behaviour when represented against the effective wind velocity (figure 2.4).

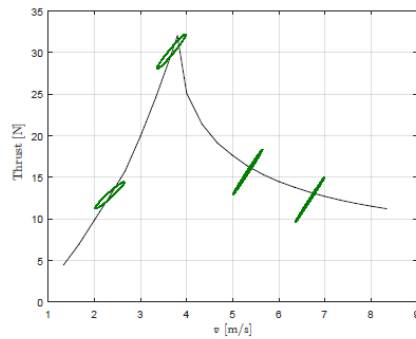


Figure 2.4: Unsteady results over static curve

Finally a validation of the AeroDyn module of FAST was carried out. AeroDyn 14/FAST 8 was taken as reference for the numerical simulation trying to impose the identical environmental conditions. The motion has to be imposed through a force at the base of the tower

achieved to a feedback control defined as:

$$F_{base} = [K](X_{ref} - X) + [C](\dot{X}_{ref} - \dot{X}) \quad (2.2)$$

where the the matrices $[K]$ and $[C]$ are treated like input parameters. The simulations were run setting Dynin inflow model, which implements Generalized Dynamic Wake Model (GDW), suitable for representing unsteady aerodynamics.

Simulation parameter	Settings
AeroDyn time step	0.001 s
Dynamic Stall Model	Steady
Use Cm	No
Inflow Model	Dynin (GDW)
Induction Factor Model	Swirl
Tip Loss Model	Prandtl
Hub Loss Model	Prandtl
Blades	Rigid
Fixed Pitch	No controller

Table 2.3: FAST/AeroDyn simulation settings

The simulation results show the hysteretic behaviour expected from the experimental results but with some differences. The surge imposed motion tests indicate a lower slope of the hysteretic cycles (i.e. the ellipsis longer axis) for the Aerodyn simulation, while the area limited by this cycles is comparable to the measured one, except for the above rated case, in which it is lower for the numerical simulation. The pitch tests show instead discrepancies from the expected ones obtaining from the wind tunnel experiments. The differences underlined are not straightforward correlate with AeroDyn numerical implementation, but they have to be taken into account for the following AdWiMo implementation, due to the aerodynamic forces are calculated by the same FAST module with the same settings.

2.2.3 Robotic Platform

Sophisticated computational aero-hydro-elastic tools are being developed for simulating the dynamics of floating offshore wind turbines, but the reliability of such prediction tools requires experimental validation. To this end, due to the lack of a large amount of full scale data available, scale tests represent a remarkable tool [5].

Experimental tests on floating offshore wind turbines are mainly made in ocean wind-wave basins while at Politecnico di Milano, due to the impossibility to perform such tests, a complementary approach based on a 6 degrees of freedom robot has been studied. A preliminary explanation of the system will be presented here, taking into account that the design and the construction of the machine is still in progress.

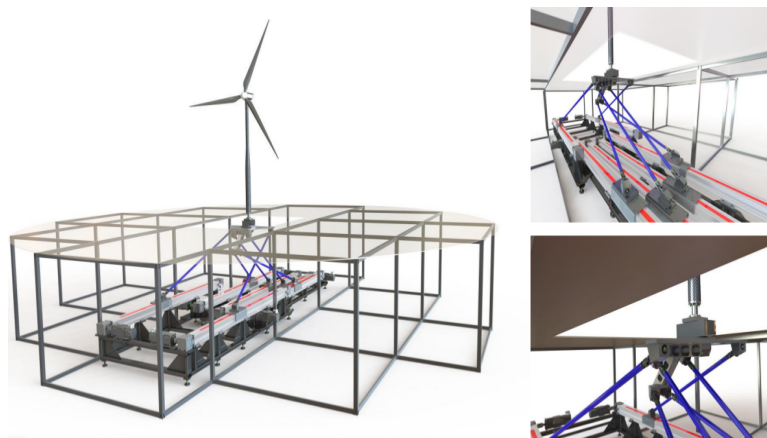


Figure 2.5: 6-Dof Robotic Platform "HexaFloat"

The design of the system has been made following 5 consecutive steps:

- definition of a total orientation workspace, accordingly with the preliminary requirements (in terms of maximum displacements and their relative maximum frequencies);
- choice of machine architecture and related geometrical parametrization;
- kinematic synthesis by multi-objective optimization of the machine dimensions, by means of a genetic algorithm (Pareto optimality);

- definition of the “best” solution by means of static and dynamic analysis of the Pareto-optimal solutions;
- mechanical sizing of the drive system and other mechanical equipments.

The family of “parallel kinematic” robots was chosen for its more suitable capabilities, compared to serial robots, in terms of high positioning accuracy (errors and backlash in serial robots are summed together amplifying their effects, while in parallel robots interact averaging), high load capacity (parallel robots have higher stiffness and they discharge loads to the ground efficiently), high dynamic performances (the actuators are mounted near the ground minimizing the mobile mass) and components modularity.

The final configuration adopted refers to the so called “Hexaglide” kinematic architecture, it is characterized by six links of fixed length, that connect the base to the mobile platform (where the scaled model of the floating wind turbine is supposed to be placed), and its motion is given by the actuation of six prismatic joints, that lay parallel to the base (figure 2.5). The robot structure will be covered when tested into the wind tunnel in order to not be subjected to aerodynamic action of the wind.

In this thesis a slightly different configuration will be modeled in AdWiMo. It is the "Hexaslide" one, where the the actuation lines are two by two parallel and each couple has 120 degrees offset (figure 2.6). It allows an higher isotropy in terms of handling [2].

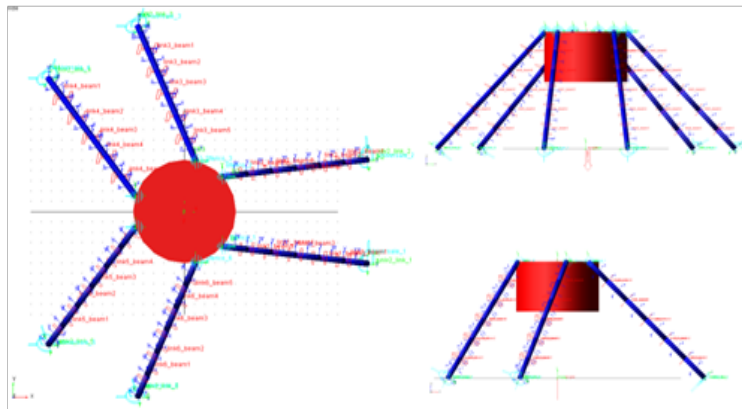


Figure 2.6: "Hexaslide" robot modeled in Adams

2.2.4 Main activities of the thesis

The objective of this thesis is to collect all the aspects that have been studied at Politecnico di Milano inside a unique numerical rig (figure 2.7) able to predict the future tests that will be performed within the LIFES50+ project.

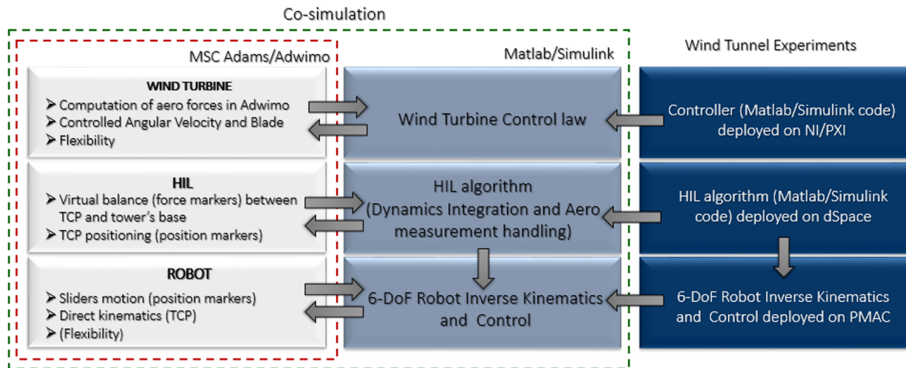


Figure 2.7: Adams/AdWiMo numerical model scheme

AdWiMo is the numerical tool chosen to achieve this goal due to the opportunity of including both the aerodynamic component from the subroutine "aerodyn13" by NREL (the same used by the previous tests made with FAST) and the handling robot through the normal features of Adams. Then the complete system will be exported to Matlab Simulink to impose the wave motion to the turbine.

First of all the red block presented in figure 2.7 has been modeled, the structural design of the turbine is created using the tools made available by AdWiMo. All the bodies can be modeled both as rigid and as flexible parts, for this work the flexibility has been exploited to calculate the modes of vibration of the system, but all the dynamic simulations have been carried out under the hypothesis of rigid bodies.

The necessity of having a constant rotor speed and blade pitch angles has been studied in detail, and different solutions will be shown.

Then the hexapod robot has been added to the wind turbine, it is accountable of the system motion that can be calculated through an inverse kinematic method starting from the desired displacement of the turbine.

The green block of figure 2.7 represents the final test rig in Simulink environment, where the hydrodynamical model has been added to the AdWiMo system. The sea state has been imposed to the turbine through the motion

of the robot, trying to reproduce faithfully the HIL (Hardware in the Loop) hybrid approach used in the wind tunnel experiments.

The thesis work has been completed by a simulation campaign in order to validate first of all the AdWiMo model of the wind turbine, and then the complete rig, comparing the results with the ones obtained in the wind tunnel at Politecnico di Milano.

The final model will be used for testing the future developments of the project (turbine control, 6-DoF motion of the system, ...) and predicting the results of the experimental campaign in the wind tunnel.

Chapter 3

Modeling

The chapter presents all the steps made for the creation of the numerical test rig in the Simulink environment.

It is interesting to see that the final model is a co-simulation between three different numerical tools. FAST describes and models the aerodynamic component, AdWiMo shapes the structural properties of the wind turbine and the hexapod robot, Simulink imposes the motion to the actuators of the moving platform.

The co-simulation between FAST and AdWiMo is developed automatically by the Adams plug-in through the subroutine "aerodyn13", while the final implementation of the model in the Simulink environment has been made during the advancement of the work and it has been one of the more difficult task to be performed.

A guide for the creation of the model in AdWiMo environment is presented in the Appendix A. It is more generic in terms of how the model is designed, what hypothesis have been made during the thesis and the relative difficulties encountered, but it explains more in detail all the passages that the user have to do, like a kind of manual.

3.1 AdWiMo environment

Adwimo, an acronym for Advanced Wind Turbine Modeling, is a plug-in of Adams, which is a multibody dynamics program built by MSC Software.

The tool allows fast modeling and accurate system simulation of wind turbines considering every major aspects of the design, including the creation of the different bodies (tower, blades, hub, ...) that compose the system,

the aerodynamic forces and different types of control (generator, pitch, yaw) [13].

The tool takes as inputs five text files containing geometric, structural and mass properties of the bodies composing the system.

The tower and the blades information are collected inside .tbb and .bbb files and modeled like flexible parts by tower_by_beam and blade_by_beam Nastran processors, considering them like discrete bodies.

The input data regarding hub, mainshaft, mainframe and generator are stored inside .hsp and .mgp files, also in this case they are considered flexible bodies but with inertia invariant set to 'rigid'. The software, further them, automatically creates, with these information, others dummy rigid bodies in the nacelle zone that constitute parts like gear box and generator-frame.

Adwimo then writes for each input a binary file (.mnf) that has to be inserted in the main properties file (.gsp) and that are accountable for the final formation of the turbine.

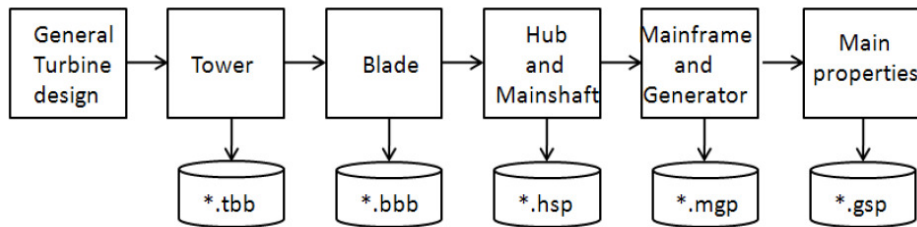


Figure 3.1: Adwimo input and data flow [13]

Regarding the aerodynamic forces applied on the blades, they are calculated using the external application named 'aerodyn13'. This modulus is part of FAST (Fatigue, Aerodynamics, Structures and Turbulence), a numeric code developed by NREL. The loads (forces and torques) are applied along the blades, acting on nodes that have been defined in another text file (.ipt) containing also the aerodynamic profiles of each section.

The normal features of Adams remain accessible and can be used to set up control, displacements, forces and constraints.

Finally, to be able to model a scaled turbine, a group of macros has to be added to the code at the start of the work. In fact, Adwimo was thought for full scale wind turbines and it has difficulties in the calculation of mass

	Name	Type
	tower	flexible
	blades	flexible
	hub	flexible (set to rigid)
main bodies	mainshaft	flexible (set to rigid)
	mainframe	flexible (set to rigid)
	generatorframe	flexible (set to rigid)
	nacelle	rigid
	foundation	rigid
dummy bodies	gear box, HSS, ...	rigid

Table 3.1: List of the bodies created in Adwimo

properties of the dummy bodies. A widespread problem encountered was the presence of singular inertia matrices of these particular elements. The macros were provided by MSC Software and act directly on the software.

Before the beginning of the construction of the system, it is useful to have a proper database in which store the inputs and where Adwimo saves all the files produced by itself. This procedure consists in the creation of a folder in which insert a copy of Adwimo (changing in its property menu the file path into `%HOMEDRIVE%%HOMEPATH%%cwd%`) and the text files for the creation of the turbine.

Then in the software screen select

Adwimo->Database Management->Create Database
Adwimo->Database Management->Set Default Writable

This command creates a folder inside the previous one where Adwimo will save the .mnf files needed to create turbine, and where the files about wind and airfoil profiles have to be stored.

3.2 Scaled Wind Turbine

In this section the steps for the creation of the scaled wind turbine in Adwimo environments will be shown following the classical procedure described in the manual but focusing on the characteristic aspects of Polimi turbine.

The LIFES50+ 10 MW scaled turbine is obtained scaling the reference DTU full-scale turbine through the following factors acting on length and speed:

$$\lambda_L = \frac{1}{75} \quad \lambda_V = \frac{1}{3}$$

and then obtaining the ones related to the other physical quantities.

Quantity	Unit of measure	Value
Frequency	[s ⁻¹]	25
Mass	[Kg]	2.37e-6
Inertia	[Kg m ²]	4.21e-10
Force	[N]	1.98e-5
Torque	[N m]	2.63e-7
Stiffness	[N m ²]	3.51e-9

Table 3.2: Scaling factors used for creating the AdWiMo turbine

All the parameters describing the Polimi scaled turbine are previously obtained and used for the creation of FAST model, and generally they have been re-utilized for creating the AdWiMo input files. The main differences regards how the software creates the turbine, FAST uses a modal approach while for AdWiMo a kind of FEM analysis is made with the discretization of the main elements of the turbine.

3.2.1 Tower

The input file (.tbb) for the tower is composed of two mainly sections described in the table 3.3.

The idea, on which this type of modeling is based, is to define the geometry of the tower like a sum of hollow truncated cones one above the other (figure 3.2). The mass of the tower is calculated as the addition of the point masses,

defined for each section, plus the non-structural mass per unit length plus the mass obtained multiply the density (of steel) for the volume of each section. In this case both the point masses and the non structural one were set to zero.

SHAPE	Section	Number of sections in which the tower is divided
	Height	The z coordinates of each section
	Outer Diameter	The external diameter of each section
	Point Mass	Concentrated mass of the section
SECTION	Wall Thickness	Thickness for each section
	Non-structural Mass	Mass per unit length for each section

Table 3.3: Parameters of the tower input file

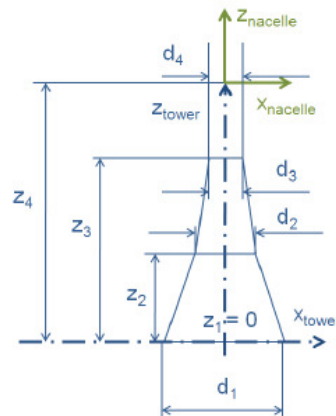


Figure 3.2: Geometry of tower [13]

The input file has been then completed with the length of the outer diameter and the wall thickness simply scaling them from the full scale model. Although the dimensions and the mass of the tower were correctly modeled, the modes of vibration and their natural frequencies did not match

the expected ones. The solution to this problem was to compare both mass (per unit length) and flexural rigidity of full scale and model scale tower.

$$\begin{cases} \frac{(EJ)_{modelscale}}{(EJ)_{fullscale}} = \lambda_L^4 \lambda_V^2 \\ \frac{(m)_{modelscale}}{(m)_{fullscale}} = \lambda_L^2 \end{cases} \quad (3.1)$$

In the system 3.1 the E is the Young's Modulus of the material (steel for both models), the J is the moment of inertia and m is the mass per unit length.

Expanding the terms, it ended up with a non-linear system with two unknowns, the inner and outer diameter of the scaled tower, in two equations function of the diameters of the full scale tower and the scaling coefficients.

$$\begin{cases} D_{e_{modelscale}}^4 - D_{i_{modelscale}}^4 = (D_{e_{fullscale}}^4 - D_{i_{fullscale}}^4) \lambda_L^4 \lambda_V^2 \\ D_{e_{modelscale}}^2 - D_{i_{modelscale}}^2 = (D_{e_{fullscale}}^2 - D_{i_{fullscale}}^2) \lambda_L^2 \end{cases} \quad (3.2)$$

Solving the system 3.2 for each section of the tower, the input file can be finished adding the outer diameter and the wall thickness t , obtained with equation 3.3.

$$t = \frac{1}{2}(D_{e_{modelscale}} - D_{i_{modelscale}}) \quad (3.3)$$

The final version of .tbb file can be seen in the Appendix C and it has to be inserted in Adwimo following the command

Adwimo->Preprocess Turbine->Preprocess Tower

3.2.2 Blades

Blades are defined in Adwimo like the sum of different airfoil profiles each one with different properties. The software creates two different coordinate systems (figure 3.3), one called blade reference frame and the other cross section reference frame (CRS). The first one is referred to the full blade profile, whose root is the origin of the system. The second one is defined for all the different sections of the blade and it is used as basis for the definition of all sectional and inertial properties. The origin of each CRS system compose

Height	1.5417 m
Mass	1.3086 Kg
Mass Inertia Tensor	$I_{xx} = 0.8078 \text{ Kg m}^2$
	$I_{yy} = 0.8078 \text{ Kg m}^2$
	$I_{zz} = 0.0003 \text{ Kg m}^2$

Table 3.4: Scaled tower properties

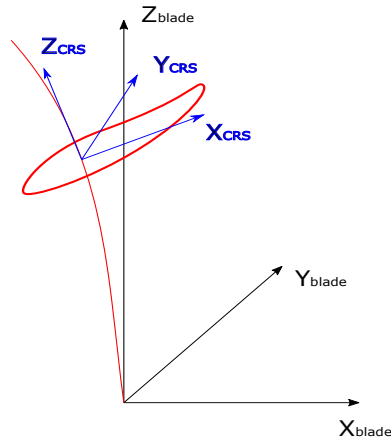


Figure 3.3: Blade and CRS reference frames [13]

the centerline of the blade.

The input file (.bbb) for blades is far more complex than the one needed for the tower, it contains four different sections with many parameters to be defined. Although this, the creation of the file is simpler than the one for the tower due to the fact that, inside it, there are information about both geometry, mass and stiffness, and then there is not the necessity of scaling the dimensions taking into account the modes of vibration as made previously for the tower input file, so they were just scaled using the proper coefficients from the reference blade of the 10MW DTU turbine .

As said in Chapter 2, the impossibility of matching the Reynolds number between the real situation and the wind tunnel had imposed the necessity of a particular design of the blade profile with respect to the DTU ones. This

implies that the chord, the twist and the relative thickness of the blades have different design to ensure the equivalence of the thrust force. This three parameters have been obtained from the FAST input files through an interpolation in the points of interest for AdWiMo (figure 3.4).

In the following tables the four sections will be briefly presented and explained. For all of them, the first two columns are the number of the section, that is the cross sectional counter, and the blade length, that is the z position of CRS frame in the blade system coordinate, so they will be omitted in the lists.

Blade geometry		
name		units
CHORD.LENGTH	absolute length of airfoil chord	[m]
REL.THICKNESS	relative thickness of airfoil	0<value<1
REL.POSITION	airfoil leading edge position	0<value<1
AIRFOIL.ORIENT	airfoil orientation	[degrees]
X.CROSS.REF	x position of CRS frame in the blade system	[m]
Y.CROSS.REF	y position of CRS frame in the blade system	[m]

Table 3.5: Blade geometry data block [13]

Blade mass		
name		units
MASS	mass per length	[Kg m ⁻¹]
POLAR.MOMENT	polar moment of inertia per length	[Kg m]
ANGLE.INERTIA	angle for mass coordinate system	[degrees]
FLAP.I-MOMENT	flapwise moment of inertia per length	[Kg m]
EDGE.I-MOMENT	edgewise moment of inertia per length	[Kg m]

Table 3.6: Blade mass data block [13]

Blade stiffness		
name		units
ANGLE.PRIN.ST	angle for principle stiffness	[degrees]
FW.BEND-STIFF	flapwise bending stiffness	[N m ²]
EW.BEND-STIFF	edgewise bending stiffness	[N m ²]
TORSION.STIFF	torsional stiffness	[N m ²]
AXIAL.STIFF	axila stiffness	[N]

Table 3.7: Blade stiffness data block [13]

Blade axis		
name		units
X.AERO	x position of aerodynamic centre in CRS frame	[m]
Y.AERO	y position of aerodynamic centre in CRS frame	[m]
X.POS.SHEAR.C	x position of shear centre in CRS frame	[m]
Y.POS.SHEAR.C	y position of shear centre in CRS frame	[m]
X.POS.CoG	x position of centre gravity in CRS frame	[m]
Y.POS.CoG	y position of centre gravity in CRS frame	[m]
X.POS.NEUTRAL	x position of neutral axis in CRS frame	[m]
Y.POS.NEUTRAL	y position of neutral axis in CRS frame	[m]

Table 3.8: Blade axis data block [13]

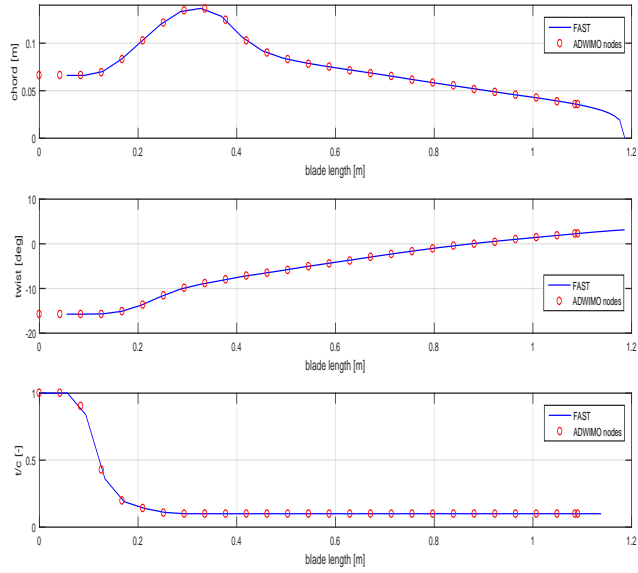


Figure 3.4: Interpolation nodes for chord, twist and relative thickness of the blades

The final version of .bbb file can be seen in the Appendix D and it has to be inserted in Adwimo following the command

Adwimo->Preprocess Turbine->Preprocess Blade

The scaled blade can be seen in figure 2.4 while its properties are presented in table 2.9.



Figure 3.5: Comparison between real and AdWiMo scaled blade

Length	1.1529 m
Mass	0.2898 Kg
Mass Inertia Tensor	$I_{xx} = 0.0763 \text{ Kg m}^2$
	$I_{yy} = 0.0763 \text{ Kg m}^2$
	$I_{zz} = 6.6e-5 \text{ Kg m}^2$
	$I_{xy} = 2.9e-6 \text{ Kg m}^2$
	$I_{yz} = -4.4e-5 \text{ Kg m}^2$

Table 3.9: Scaled blade properties

3.2.3 Hub, Mainshaft, Mainframe and Generatorframe

In this section the modeling of the nacelle will be briefly described. Adwimo creates four principal flexible bodies, the hub and the mainshaft with the input file .hsp, the mainframe and the generatorframe with the file .mgp. In addition of those elements, the software models some rigid bodies in this zone of the system that are not directly defined by the user in the pre-process phase.

In the two files some information are contained, regarding mass and inertia properties of the bodies and position of the bearing nodes that are used as references for the creation of the other bodies.

The compilation of the input files was simply made by scaling the parameters needed, starting from the input files of the full scale turbine. Then they have been inserted in Adwimo following the instructions

Adwimo->Preprocess Turbine->Preprocess Hub and Mainshaft
Adwimo->Preprocess Turbine->Preprocess Main- and Generatorframe

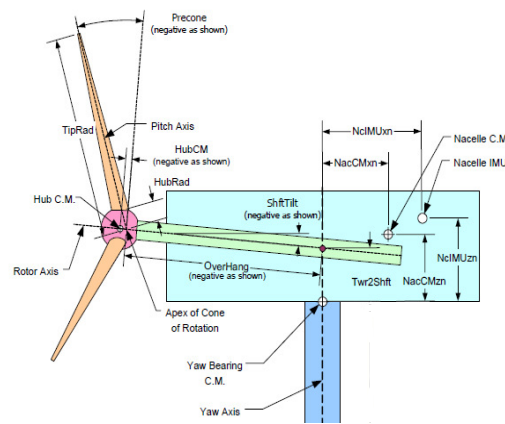


Figure 3.6: Layout of the nacelle zone [9]

3.2.4 Creation of the turbine

The previous steps are responsible for the creation of the binary Nastran files needed for the creation of the turbine. Those files, whose extension is .mnf, have been collected inside the folder *flex_bodys.tbl* present in the work

database.

The next procedure consists in making another text file (.gsp) containing the path of the location of the .mnf inputs plus other information regarding the numeration of the nodes of the bodies, the platform on which the turbine will be created and the overhang (see figure 3.6).

The final version of the properties input file has to be inserted in Adwimo following the command

Adwimo->Preprocess Turbine->Create Turbine Property File

The assembling of the turbine is then completed by the command

Adwimo->Create Turbine

that opens a dialog box in which the turbine property file has to be included.

Adwimo creates the model but it shows some errors regarding mass properties of the rigid bodies created in the nacelle zone (*hss_lumpmass, generator_hss, generator_rotor, generator_stator, lss_lumpmass, GEAR_BOX, HSS, LSS, fix_lumpmass, nacelle*). For the solution of this problem another wind turbine was generated, the NREL 5MW full-scale, that is the reference example for Adwimo, and then all the masses and the inertia tensors needed were saved. Having those parameters, they were up-scaled to be coherent with the DTU 10MW turbine and then down-scaled to meet the requirements of our model. The scaling coefficients for passing from the 5MW turbine to the 10MW turbine are

$$\lambda_L = \sqrt[3]{2} \quad \lambda_V = 1$$

Regarding the platform, it is a fundamental body for Adwimo, that can not work without it, but it is useless for the Polimi application (future addition of the robot). In order to overcome this complication, its mass and inertia were set to zero and it has been made invisible.

Another problem encountered concerns a connector between the hub and the mainframe. The fixed joint was opened due to the misalignment of the two markers, one for each body, the bond was composed of. Changing the position of the passive node, and placing it equal to the one of the active marker, was the solution that closed the connector.

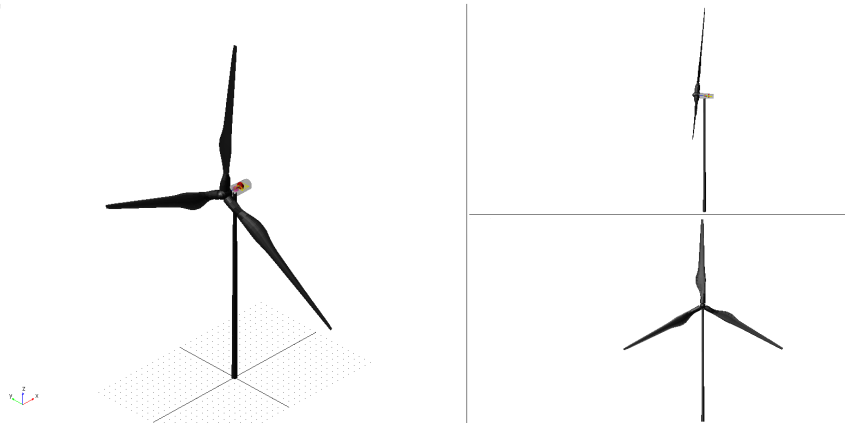


Figure 3.7: Scaled wind turbine in Adwimo environment

Mass	3.1133 Kg
Center of Mass Location	$x = -1.2e-2$ m
	$y = 5.8e-4$ m
	$z = 1.1285$ m
Mass Inertia Tensor	$I_{xx} = 4.9952$ Kg m ²
	$I_{yy} = 4.9698$ Kg m ²
	$I_{zz} = 4.1e-2$ Kg m ²
	$I_{xy} = 1.0e-4$ Kg m ²
	$I_{zx} = -5.6e-2$ Kg m ²
	$I_{yz} = 2.9e-3$ Kg m ²

Table 3.10: Scaled turbine properties

3.2.5 Aerodynamic forces

The main characteristic of the Adwimo tool is the possibility of a co-simulation with FAST that gives to the user the possibility of a quick and easy modeling of the aerodynamic forces.

The software can set the aero-forces on blades, on tower and on nacelle but for this application only the first ones have been applied.

The aerodynamic forces acting on the blades are calculated in Adwimo using the external application *aerodyn13* developed by NREL. The configuration of the data for the loads has to be collected in an *.ipt* input file inserted in the folder *aerodyne.tbl* located in the work database. It is identical to the input file needed for the simulation with AeroDyn previously made. This file is read by Adwimo with the command

Adwimo->Set Aero Forces->Blade

Having modeled the blade as a discrete body made up by different section with different structural properties, also the aerodynamic loads are applied on some nodes positioned along the blade (the nodes for the structural modeling could be different from the ones needed for aero-forces). For each node the software calculates the force and the torque using the information contained in the *.ipt* file.

Inside it, the type of the mathematical design for the calculation of the aerodynamic forces has been set (equals to the ones set for AeroDyn simulation in table 2.3); furthermore the conditions of the air are present. The wind condition and the airfoil properties require other text files, so the *.ipt* file recall the path for them.

The wind is described inside a *.wnd* file in the specific folder *wind.tbl*, it contains the temporal story of the wind including speed, direction and shear. For this application only constant speed wind was used with perpendicular direction compared to the rotor axis.

The airfoil profiles input files are collected inside the folder *airfoil.tbl*, one profile for each node in which the blade is divided.

An example of the aerodynamic forces calculated with FAST can be seen in the Appendix E.

3.2.6 Rotor control

Adwimo allows different types of control acting on different aspects of the turbine. All the controllers may be modeled either individually or as a whole closed loop control system.

In this application there was the necessity of working with constant rotor speed and with a precise constant pitch angle of the blade in function of the wind speed.

Regarding the last aspects Adwimo supports a pitch controller that set the angle to the desired value at the beginning of the simulation and then kept it constant for all the duration.

For the rotor speed two different types of solution were implemented, obtaining the same result but with different transient and, above all, with different consequences on the possibility of a good co-simulation with Simulink.

The first solution was to implement a PI (proportional and integral) control loop feedback mechanism that gives as output the torque to be applied on the rotor in order to have the reference angular velocity.

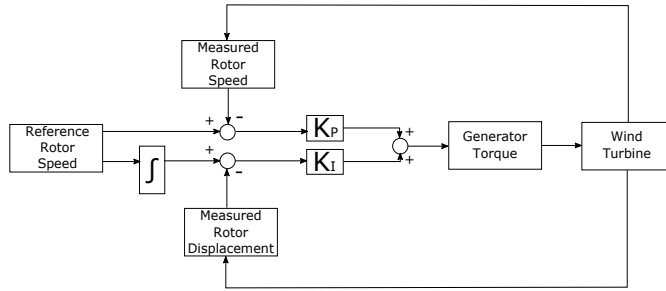


Figure 3.8: Rotor control logic

The generator torque, in Nm , is defined as

$$T = K_P(\omega_R - \omega) + K_I(\theta_R - \theta) \quad (3.4)$$

where $(\omega_R - \omega)$ is the error between, respectively, the reference and the measured rotor speed, in rps (rounds per second), while $(\theta_R - \theta)$ is the error between the reference and the measured rotor angular displacement, with no unit of measure. The gains of the controller are set equal to

$$K_P = -0.2655 \frac{Nm}{s} \quad K_I = -0.527 Nm$$

In Adwimo it has been realized using the command

Adwimo->Set Controller->Generator Controller

and selecting in the dialog box *Runtime_function*, completing it with a formula, in Adams language, equivalent to the equation 3.4.

The second solution was to impose a constant rotor speed with a rotational motion, defined in velocity, between the stator and the rotor. The motion has been defined as

$$\left(\frac{2\pi\omega_R}{60}\right)50step(time, 5, 0, 5.1, 1)$$

where the term between the brackets is the reference angular speed expressed in $\frac{rad}{s}$, followed by the gear box ratio and a step function, added in order to meet the Adwimo convention for which the aerodynamic forces start after five seconds of simulation.

The gear box ratio is set up using the following command

Adwimo->Set Gear Box->Set Gear Box Ratio

Although the final result is similar, the implementation of one of the two solutions gives different consequences respect to the other one. The imposed motion has zero overshoot and its steady state error is null, while the implementation of the PI control logic has a longer transient time and an oscillating steady state condition. In order to overcome these problems the control gains have to be big enough, in absolute value, like the ones that have been set, but this decision leads to a very high overshoot. It means that the rotor speed is extremely high for a short time interval, and it causes the displacement of the system from the equilibrium position.

In conclusion the imposed motion has been used for the simulations in the Adwimo environment because it gives the best results, but for the co-simulation with Simulink it was necessary to work with the PI control logic, as it will be explained in detail in the co-simulation section of the thesis, paying attention to let the system return to the equilibrium position before starting the desired simulation.

3.3 Robot

The "Hexaslide" robot has been firstly modeled in Adams for the flexibility analysis during the LIFES50+ project. The task performed inside this thesis was to add the robot to the scaled wind turbine created with AdWiMo. The design of the machine can be seen in figure 2.6, it is composed by a platform made up by a rigid cylindrical body, six flexible links of equal length

and six sliders modeled like six parallelepipeds.

The platform can be considered like a rigid body because it is made up of a set of aluminum plates with appropriate ribs to counter the inflection of the plates, so as to have a structure that is both rigid and light at the same time (figure 3.9).

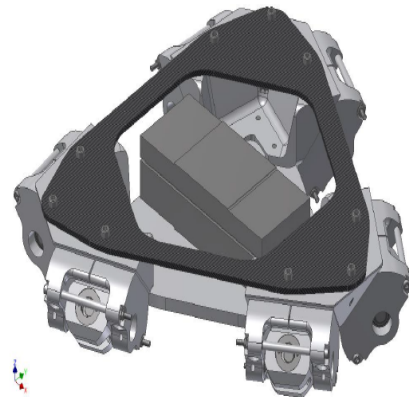


Figure 3.9: CAD model of the platform

The flexible links are modeled like a sum of smaller rigid hollow cylindrical parts connected by a force field used for simulating the axial, the flexional and the torsional stiffness of a beam. The simulations made during this thesis hypothesize a completely rigid system, then the links have been simply made by only one rigid cylinder.

The inertial contribution of the sliders has been overlooked.

The previous flexibility analysis gives the final inertial data of all the robotic system, summarized in table 3.11.

To constrain, the system ideal joints have been considered. Six spherical joints (allow rotation and prevent translation) connect each link to the platform, six universal joints (transmit rotary motion) relate links and sliders, finally six prismatic joints fix the sliders to the ground permitting only the translational motion along the slider guide.

The actuation of the prismatic joints, combined with the other constraints and the geometry of the robot, allows the 6-DoF motion of the platform.

Both for the design phase and for the flexibility analysis two reference markers have been kept in consideration: the origin of the coordinate system of

	mass	32.828 Kg
platform	Ixx	0.557 Kg m ²
	Iyy	0.608 Kg m ²
	Izz	1.060 Kg m ²
slider	mass	5.388 Kg
link	length	0.484 m
	mass	3.632 Kg

Table 3.11: Inertial parameters of "Hexaslide" robot

the space of work, automatically created by Adams, and the Tool Center Point (TCP), the center point on the upper surface of the platform. They represent respectively the fixed reference frame and the moving one.

All the other markers used for bodies, constraints and forces have been parametrized in such a way that if the coordinates of the TCP changes, every elements of the robot will move in the new configuration. This consideration has been used also for the creation of the complete system (wind turbine plus hexapod robot).

The addition of the "Hexaslide" robot to the scaled wind turbine has been performed through the creation of a macro written in Adams "language" and then red by AdWiMo.

The macro consists in the following steps:

- parametrization of all the markers of the scaled turbine bodies respect to the origin of the system, this passage allows to an easier construction of the connection of the turbine with robot;
- creation of the TCP marker, needed to define the center of mass of the platform and the measures of the displacements of the turbine base;
- creation of the "wind tunnel floor" marker, it creates the plane that simulates the wind tunnel floor under the robot platform needed to define the sliders bodies;
- creation of the platform rigid body and definition of its inertial properties and center of mass;

- creation of the link bodies, specifying if they are composed by a single (rigid body) or multiple parts (flexible body);
- creation of the slider bodies;
- creation of all the constraints described in the previous paragraph;
- creation of the translation motion needed to move each slider.

The final complete model in AdWiMo environment can be seen in figure 3.10.

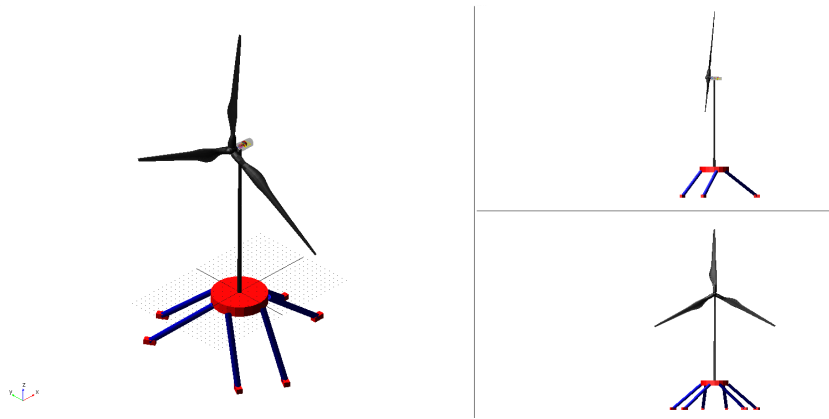


Figure 3.10: Turbine-robot system in Adwimo environment

To perform the simulations, the desired motion at the base of the turbine will be imposed through the linear motions of the sliders, like what happens in the real experimental tests in the wind tunnel, where the motion of the turbine will be performed through the actuation of the six motors of the robot.

An inverse kinematic approach is necessary to calculate the sliders motion. It is made with a Matlab function that takes as input the desired motion at the base of the turbine, made by three linear components along the x-y-z axes (surge-sway-heave) and the relative rotations (roll-pitch-yaw), and gives the six motions of the sliders. They are calculated through the definition of some geometrical parameters (related to the links and the equilibrium position of the robot in steady state) and a rotational matrix made with the angle convention (nautical x-y-x angles).

The final displacements of the sliders are imported in AdWiMo through a

cubic-fitting interpolation spline method. In order to achieve the continuity until the accelerations, the motion at the sliders is imposed in velocity.

3.4 Co-simulation in Simulink environment

The necessity of simulating the wave loads through the motion of the robot made inevitable the co-simulation in Simulink environment of the system. AdWiMo allows the transfer of a model in Matlab Simulink environment through a plug-in named "Adams Control". It permits the creation of a Simulink block in which all the AdWiMo model is contained, defining the inputs and the outputs of this block as Adams state variables.

The plug-in creates many text files that will be read by the Matlab simulation. The most important is the .adm file which contains all the information about the AdWiMo model, starting from the definition of the bodies, constraints and forces to the type of numerical solver that will be used for the simulation.

At each time interval the Simulink model will provide the input to the Adwimo block, which will perform the aero-elastic simulation and will give the desired output to Matlab.

During the development of the thesis some expedients have been taken into account for a good and correct simulation.

First of all, the time interval of the Simulink model has to be equal or less than the integration step of the AdWiMo solver, otherwise the two software are not able to communicate and the simulation will be aborted.

Regarding the solver, AdWiMo allows different kinds of dynamic solvers but the choice of one of them conditions the results of the Simulink simulation. Many "empty" co-simulations were performed simply imposing a sinusoidal surge motion and varying the type of solver, the integration time step and the error allowed. The results have then been compared with the outputs obtained, with the same simulation settings, in AdWiMo environment. For this thesis the GSTIFF solver has been considered as the best solution in terms of time consuming and result precision. The GSTIFF integration method, developed by C. W. Gear, is a variable order, variable step size integration method that uses a backwards difference formulation.

Another important consideration is related to the typology of the AdWiMo input. Generally it has been seen that imposing forces and torques gives better results than imposing motions. It is not possible for this application to apply only forces because the hydrodynamic state has been designed as an imposed motion at the base of the turbine. Concerning the imposed rotor

speed, as said in the previous section, the best solution was to directly place a velocity motion between stator and rotor. This method does not work if the simulation will be performed in Simulink environment, while imposing a rotor torque, calculated with a proper control logic, gives correct results after a short transient.

Finally the motion at the sliders has been imposed in term of speed in order to have a continuity of setting with respect to AdWiMo, although in this case there is no more the spline interpolation.

For this thesis a set of fixed inputs and outputs have been chosen and are listed in table 3.12. The final Simulink scheme containing the wind turbine plus the hexapod robot is shown in figure 3.11, where are indicated all the inputs and outputs of the system and the rotor control logic. The orange block is directly built by AdWiMo through the "Adams Control" plug-in.

input	slider motions [m/s]
	blade pitch angles [deg]
	control rotor torque [Nm]
output	TCP displacements [m]
	TCP rotations [rad]
	reaction forces at tower base [N]
	reaction moments at tower blades [Nm]
	thrust force [N]
	rotor torque [Nm]
	rotor angular displacements [rad]
	rotor angular velocity [rad/s]

Table 3.12: Inputs and outputs of the Simulink block

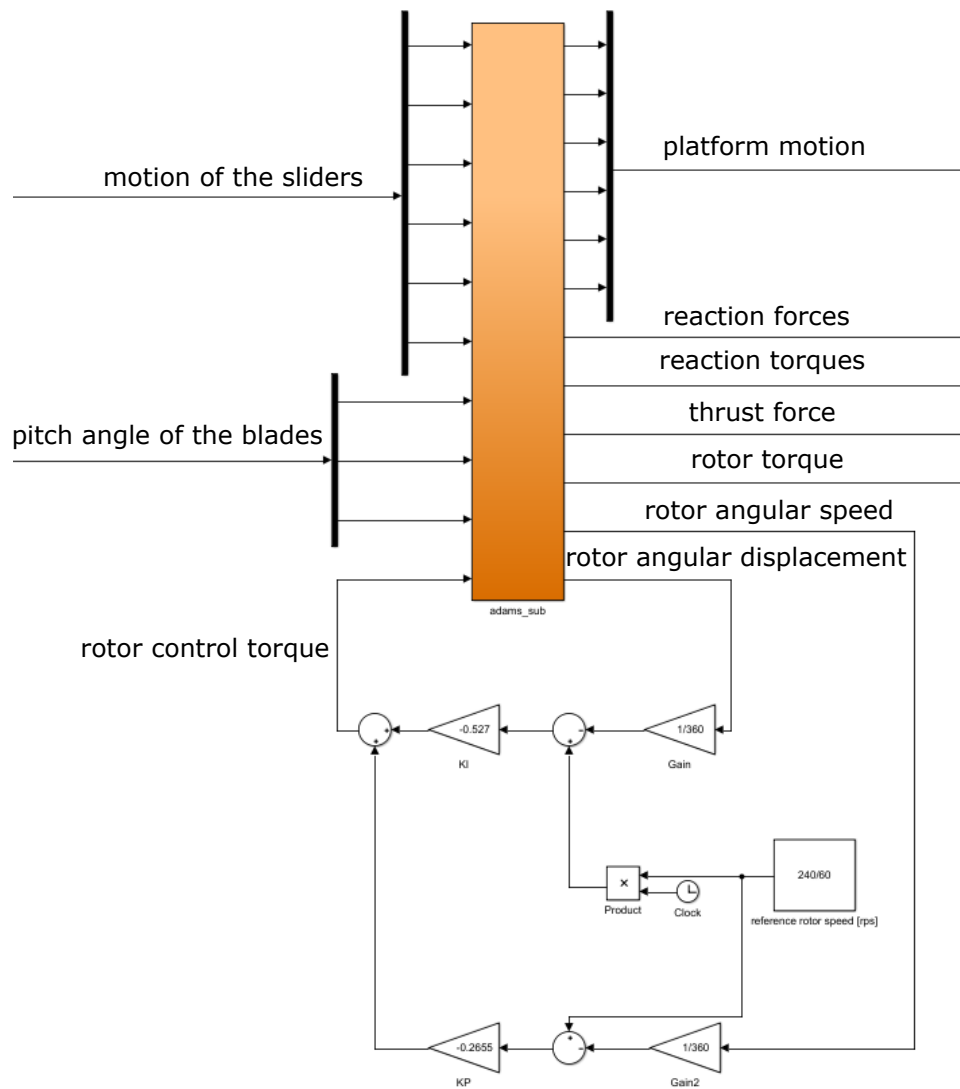


Figure 3.11: Simulink model of the AdWiMo system

Chapter 4

Validation of the model

In this chapter the preliminary simulations made for the validation of the AdWiMo model will be presented.

First of all a modal analysis has been made for evaluating the modes of vibration of the scaled turbine, both in the case of the purely scaled DTU 10 MW wind turbine and in the case of the Polimi one.

Then the same simulations that have been performed for validating Aero-Dyn (described in Chapter 2) have been carried out, analyzing the same aspects in order to make a clear comparison both with the numerical results of FAST and with the experimental results obtained in the wind tunnel.

The steady tests will be presented, showing the performances of the scaled turbine in terms of thrust and torque, and comparing them with the expected values of the DTU 10 MW wind turbine (properly scaled with the force and torque coefficients).

Finally some unsteady simulations have been made in order to analyze the influence of an imposed sinusoidal surge motion, varying both its amplitude and frequency, on the thrust and torque parameters. These tests have been carried out varying also the wind condition, and the results have been studied considering the mean values and the amplitude variations of the desired quantities. Then the obtained hysteresis cycles have been compared with the ones obtained with FAST.

All the simulations described have been made in AdWiMo environment only, not considering the possibility of the Simulink co-simulation, because they have been thought for the validation of the software itself. Despite this, the results obtained have been used also for verifying the correctness of the future co-simulation.

One important consideration has to be made before starting the analysis of

the tests made. In the steady and unsteady simulations there are not differences on testing the scaled 10 MW turbine or the Polimi one in terms of structural design, because they were carried out considering a full rigid system subjected to the same aerodynamic forces (moreover, for the unsteady simulations, the inertial effects have been properly eliminated). Naturally this consideration can not be made for the modal analysis.

4.1 Modal analysis

A modal analysis is necessary before starting the aerodynamic simulations in order to verify if the discrete modeling of the AdWiMo bodies has been correctly made.

The software allows the calculation of the modes of vibration with a simple simulation, using the following command:

```
> sim/ini  
> lin/eigen
```

that gives as output the proper frequencies of the system and the animation of the modes.

The analysis has been carried out considering only the scaled turbine without the robot, in order to have a simpler system whose modes of vibration can be compared to the ones previously obtained from the DTU turbine.

The bodies have been considered flexible, in particular the blades and the tower (the nacelle zone was set as flexible where it was possible, but the hypothesis of considering it rigid gave the same results). The tower has been constrained to the ground with a fixed joint.

The aerodynamic component has been set to zero, considering a no-wind situation (so no aerodynamic forces) and a null rotation of the rotor.

Initially the the purely scaled turbine obtained from the 10 MW DTU one has been considered, in order to understand if AdWiMo is able to determine the modes of vibration in a correct way.

The obtained frequencies have been compared to the one of the full-scale turbine properly scaled with the frequency factor:

$$\lambda_f = \frac{\lambda_V}{\lambda_L} = 0.04$$

mode	reference frequency [Hz]	AdWiMo frequency [Hz]
1 st tower SS	6.2128	6.2488
1 st tower FA	6.2858	6.2882
1 st drivetrain	12.556	20.793
1 st blade asym. flapwise yaw	13.676	14.021
1 st blade asym. flapwise tilt	14.753	15.149
1 st blade collective flap	15.849	15.922
1 st blade asym. edgewise 1	23.051	23.611
1 st blade asym. edgewise 2	23.394	23.939
2 nd blade asym. flapwise yaw	34.406	36.035
2 nd blade asym. flapwise tilt	38.762	40.751
2 nd blade collective flap	44.083	45.296
2 nd tower SS	49.236	54.180
2 nd tower FA	56.168	58.100

Table 4.1: Comparison of the modes of vibration of the DTU 10 MW scaled wind turbine

The results are summarized in the table 4.1 and they show a very good correspondence between the reference frequencies of the real turbine and the ones calculated in AdWiMo, except for the drivetrain mode that results overestimated by some Hertz.

This preliminary analysis gave two important directions: the first is the fact that the creation of flexible bodies using the discretization method in AdWiMo works correctly, the second is that the structural simulation gives the right solution comparing it with the real case.

The next step was to perform the modal analysis of the Polimi wind turbine. As said in the Chapter 2, the turbine used for the wind tunnel tests is slightly different from the purely scaled DTU in order to achieve the correct Reynolds number, but the differences concern also the mass and the stiffness properties of the tower and the blades.

Using the input files for the elastic analysis made in FAST environment, the mass and inertia of tower and blades have been changed to match the proper modes of vibration of the two bodies.

In the following paragraphs the creation of the modified input file and the structural analysis will be shown separately for the tower and the blade, and then the modes of vibration of the complete turbine will be presented.

Regarding the tower, the structural design focused on three main parameters: the mass per unit length, the fore-aft stiffness and the side-to-side stiffness, each one defined for a specific section of the body. The two stiffness have been supposed equal.

Knowing how the input file for AdWiMo is made, it has been completed using the simple system of two equations in two unknowns:

$$\begin{cases} E\pi \cdot \frac{D_e^4 - D_i^4}{64} = FA - Stiffness \\ \rho\pi \cdot \frac{D_e^2 - D_i^2}{4} = Mass/Length \end{cases} \quad (4.1)$$

where E and ρ are the Young modulus and the density of the aluminum. The parameters involved in the design of the tower, and obtained from the FAST analysis, are describe in the table 4.2 and the Adwimo input file obtained is exactly the one showed in Appendix C.

section	z-coordinate [m]	mass density [Kg/m]	FA-SS-stiffness [Nm ²]
1	0.000	1.2443	4511.0466
2	0.162	1.1994	4039.6695
3	0.357	1.0868	3393.2221
4	0.553	0.9795	2826.4191
5	0.749	0.8775	2332.4760
6	0.944	0.7807	1904.9771
7	1.140	0.6891	1537.7277
8	1.335	0.6028	1224.9758
9	1.542	0.5203	953.1523

Table 4.2: Real structural parameters of Polimi turbine tower

The modal simulation made in FAST environment gave the shape of the modes of vibration of the tower in terms of the coefficients of a polynomial

curve simulating how the tower vibrates.

Having supposed the same stiffness of the tower both for fore-aft and for side-to-side modes, the shapes of the vibration related to them approximately coincide (but in a different plane) and also their proper frequencies. In figure 4.1 the first mode of vibration of the tower is presented, on the left there is the FAST polynomial while on the right the AdWiMo result, whose frequency is around 17.4 Hz. Similarly, in the figure 4.2 there is the second mode corresponding to a frequency of approximately 84.3 Hz.

The results obtained with the two software seem to coincide with less than a scale factor.



Figure 4.1: First mode of vibration of the tower

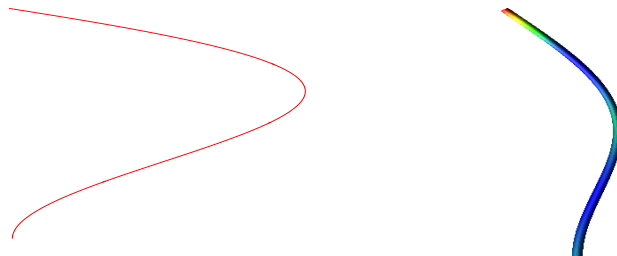


Figure 4.2: Second mode of vibration of the tower

The same considerations have been made also for the blade. As said in Chapter 3, the AdWiMo input file contains a section in which insert the mass per unit length of the blade, named *BLADE_MASS*, and one in which insert all the stiffness parameters, named *BLADE_STIFFNESS*.

Like for the tower, also for the blades the FAST input file used for the elastic

analysis have been used to obtain the data needed for the creation of the AdWiMo blade file.

In this case no further calculations were needed, but the parameters have been simply copied from the FAST file to the AdWiMo one. In the Appendix D the final formulation of the input file can be seen.

It is important to note that the only stiffness really designed is the flap-wise bending one, while the edge-wise, the torsional and the axial stiffness have been imposed equal to infinite.

For this reason, in the modal analysis, only the flap modes can be seen, and they have been compared to the expected shape formulated in the FAST file.

For the simulation made in AdWiMo environment, the blade has been constrained to the ground with a fixed joint imposed to its root, like a cantilever beam.

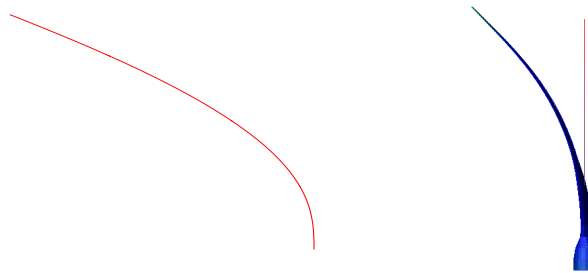


Figure 4.3: First flap-wise mode of vibration of the blade

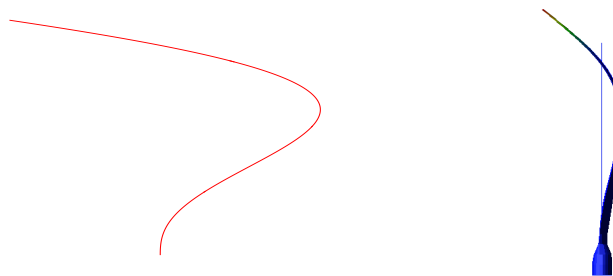


Figure 4.4: Second flap-wise mode of vibration of the blade

In figure 4.3 the first flap-wise mode can be seen, corresponding to a

frequency of 14.8 Hz, in figure 4.4 the second mode, at a frequency of 50.3 Hz.

As for the tower, the two modes are very similar to the FAST shape, unless for a scale factor.

The modal analysis made for the two bodies, considered one at time, allows the calculation of the modes of vibration of the full system Polimi turbine, like the one made for the scaled DTU.

The modal simulation has been performed in the same way, connecting the base of the tower to the ground through a fixed joint, and considering all the bodies flexible and no effects of the aerodynamic forces or of the rotation of the rotor.

During the design of the real wind turbine to be mounted in the wind tunnel, an experimental modal analysis has been made to verify the effective natural frequencies of the model. Three mode shapes were investigated, the 1st tower fore-aft, the 1st isolated blade flap and the 1st blade collective flap. The purpose of the AdWiMo analysis was to see if the software is able to perfectly match the obtained experimental frequencies.

In the table 4.3 the comparison between the target frequencies, the ones obtained with the experimental tests and the ones obtained with the numerical simulation is shown. Two main considerations can be made. The first regards the discrepancy of the target and the experimental frequencies, it is due to the design of the scaled Polimi turbine, in particular of the mass of the nacelle. The second consideration regards the comparison between the experimental and the numerical results (figure 4.5), the frequencies are similar to less than small errors of few Hertz. Also in this case, probably, the discrepancy is due to the mass of the nacelle, considering that AdWiMo creates many rigid bodies in this zone whose properties are not directly chosen by the user in the pre-process phase.

mode	target [Hz]	experimental [Hz]	numerical [Hz]
1 st tower fore-aft	6.275	5.18	4.11
1 st isolated blade flap	15.25	17.1	13.38
1 st collective blade flap	15.85	15.58	15.48

Table 4.3: Comparison of natural frequencies of Polimi turbine

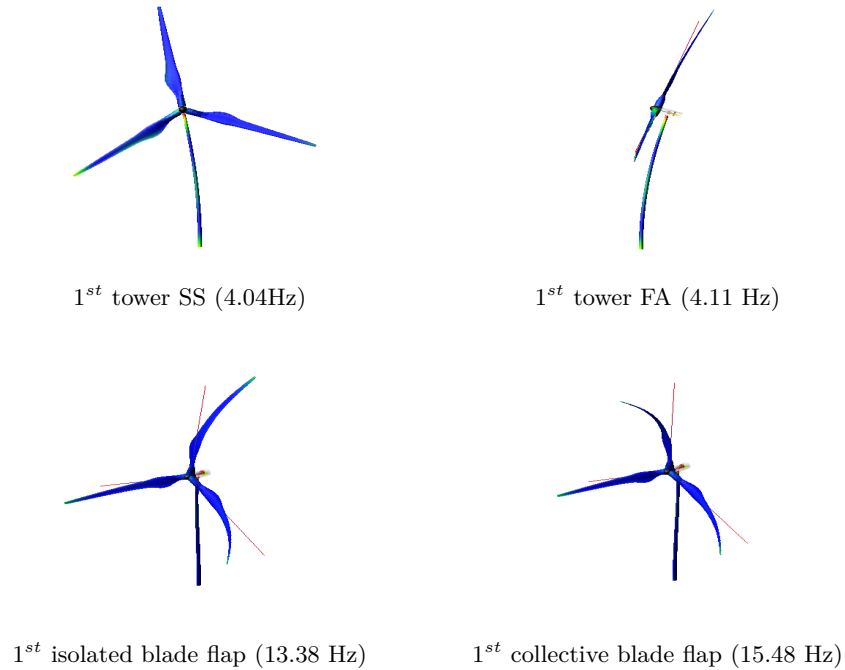


Figure 4.5: Polimi wind turbine modes of vibration

4.2 Steady analysis

In this section the results about the steady tests, aimed at characterizing the performance of the scaled turbine along the reference curve, are reported in terms of rotor thrust, torque and thrust coefficient C_t .

The purpose of this analysis is to compare the results obtained in the Polimi wind tunnel to the ones obtained in AdWiMo environment, taking into account the fact that the aerodynamic forces are calculated through the FAST subroutine *aerodyn13*.

The simulations have been carried out like the experimental tests, constraining the tower turbine to the ground through a fixed joint (in these simulations the robot has not been added to the system) and calculating the thrust and the torque varying the wind velocity until the cut-out speed.

For some specific wind velocities the pitch angle, for each blade, has been modified in order to match the desired thrust value. The reference pitch angles from the DTU 10 MW scaled turbine have been used.

The speeds of the wind and the rotor have been obtained using the velocity scale factor $\lambda_V = 3$.

Adwimo allows the dynamic simulations through the command:

Adwimo->Setup Analysis->Single Analysis (interactive)

in which the user have to define the wind input file needed for the simulation and the type of analysis wanted.

In this case the simulation script was:

```
> output/nosep
> sim/sta
> sim/tra,end=20,dtout=0.001
```

The second line is not of interest for the analysis but it is needed for AdWiMo to perform an initial static simulation. The third line is the dynamic simulation, a total time of 20 seconds has been chosen in order to eliminate the transitory introduced by the activation of the aerodynamic forces and the rotor rotation.

Like for the modal analysis, also in this case, before testing the real Polimi turbine, a preliminary set of simulations was performed on the purely scaled DTU 10 MW turbine.

Having hypothesized a full rigid system, the structure of the Polimi turbine can be used for this analysis, with the only difference regarding the *aerodyn* input .ipt file, that in this case has been obtaining simply utilizing the two scaling factors for length and speed.

The simulations have been carried out starting from the cut-in wind speed (that is equals to $1.3 \frac{m}{s}$ and characterized by a rotor speed of 150 rpm and a blade pitch angle of 2.75 deg) to the cut-out one ($8.3 \frac{m}{s}$ with rotor speed of 240 rpm and pitch angle of 22.98 deg).

The results are shown in figure 4.6. On the left-hand side the obtained thrust force is compared to the reference curve of the scaled 10 MW DTU turbine, indicating an excellent agreement, while on the right-hand side the the same comparison is made for the rotor torque. In this case the reference curve and the numerical values coincide until the rated condition, while for the above one the AdWiMo results are underestimated.

Some considerations can be made after this preliminary analysis: AdWiMo is able to perfectly describe the thrust force through the aerodynamic co-simulation with FAST, while regarding the rotor torque the above rated discrepancy can be explained by a non-perfect scaling of the blade pitch angle for this wind condition.

In conclusion the AdWiMo model can be used to test the wind tunnel forces acting to the real Polimi turbine.

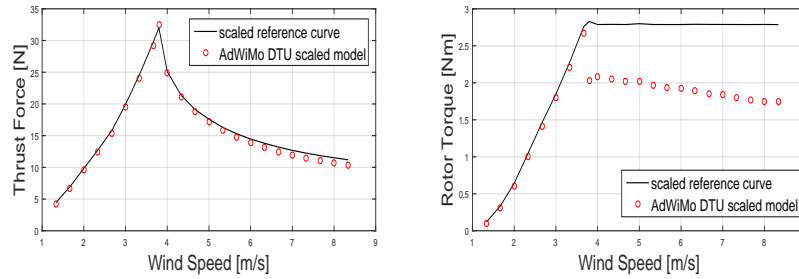


Figure 4.6: Performances of DTU 10 MW scaled wind turbine

The aerodynamic forces acting on the Polimi turbine have been calculating taking in consideration the wind tunnel parameters in which the system has been tested. The loads, calculated by FAST and utilized in AdWiMo, are exactly the ones presents in Appendix E, and they have been used for all the following analysis, both steady and unsteady.

The performances of the Polimi turbine have been calculated in the same way made for the scaled DTU turbine, testing the machine for different wind speeds and adapting the rotor rotation and the blade pitch angle in function of it. The different conditions can be seen in table 4.4.

wind speed [m/s]	rotor rotation [rpm]	blade pitch angle [deg]
2.33	150.00	0.00
2.66	160.58	0.00
3.33	200.73	0.00
3.80	240.00	0.00
4.67	240.00	9.29
5.33	240.00	12.50
6.67	240.00	17.62

Table 4.4: Wind conditions utilized for steady tests

Some considerations have to be made before analyzing the results:

- the results are plotted against the target curve obtained scaling the DTU 10 MW turbine, in reality a more correct comparison has to be made against the tests carried out in the wind tunnel (see figure 2.3);
- the simulations have been made considering the speed scaling coefficient $\lambda_V = 3$ because it is the one chosen for the following unsteady tests, but the steady performances obtained with $\lambda_V = 2$ in the wind tunnel are more similar to the target ones;
- the objective of the scaling process was to match the thrust force prior to the torque, the tests made in the wind tunnel show a good response for the torque up to the rated wind condition while for the above condition there is an high discrepancy between the two results (see the right-hand side of figure 2.3);
- the blade pitch angles used for the simulation are the ones obtained for the scaled DTU model;

The simulations have given excellent results regarding the thrust comparison with the target curve and the wind tunnel tests. In figure 4.7 the obtained thrust force and thrust coefficient are shown comparing them to the scaled DTU turbine target.

The thrust coefficient can be defined as a function of the axial induction factor and used to express the maximum thrust force upon the energy conversion device. It has been calculated with the following equation:

$$C_t = \frac{T}{\frac{1}{2}\rho A_t U_\infty^2} \quad (4.2)$$

where T is the thrust force, ρ is the air density, A_t is the rotor disc area and U_∞ is the wind speed.

The torque results are very different from the values obtained in the wind tunnel, which are in turn different from the target ones, especially for the above condition. A better comparison can be made between AdWiMo and FAST torque values, because the aerodynamic forces are calculated in the same way for each software. This analysis can be seen in the following section about the unsteady tests.

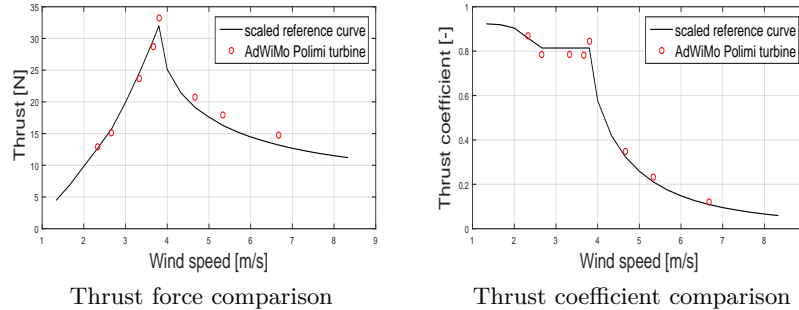


Figure 4.7: Thrust results for steady analysis on Polimi turbine compared to the target curves

4.3 Unsteady analysis

In this section the results of the unsteady simulations will be presented performing the same tests and the same analysis described in Chapter 2, speaking about the validation of the FAST module AeroDyn made at Politecnico di Milano and reported in [7].

The results of this analysis are of a great importance for the validation of the AdWiMo model because they can be compared both with the experimental tests carried out in the wind tunnel and with the numerical simulations made in FAST.

Furthermore they give a preliminary indication of what to expect from the following (it will be described in Chapter 5) implementation of the 2-DoF hydrodynamic model.

The tests in the wind tunnel have been carried out imposing a sinusoidal surge motion (transnational motion along the same direction of the wind) with different amplitudes and frequencies, and measuring the force acting on the hub of the turbine, along the same direction of the motion, and the rotor torque.

In order to have the real aerodynamic forces there was the necessity of eliminate the inertial component introduced by the motion of the turbine, so for each different surge displacement a wind and a no-wind test have been performed.

In AdWiMo the simulations have been made in the same way done for the steady ones, changing only the total time of the simulation to 88 sec-

onds, in order to eliminate the aerodynamic transient and to have a proper number of periods of motion to be analyzed.

This time the system is also made up of the robot because the sinusoidal displacement of the turbine has been imposed through the sliders. As said previously in Chapter 3, the transnational motion of the six sliders was firstly calculated by a Matlab function that takes as inputs the desired displacement of the turbine and some geometrical parameters of the robot.

The time sequences was then saved in a data file that can be red by Ad-WiMo and imposed as motion through a cubic spline interpolation. In order to maintain the continuity up to the accelerations (and so up to the inertial forces), the motion of the sliders was imposed in terms of speed.

The dynamic solver chosen for the simulation was the GSTIFF one, with a time step of 0.001 seconds and a maximum admissible integration error of 0.001.

In the table 4.5 all the simulations that have been carried out are shown, where U is the wind speed, Ω is the rotor angular velocity, F_x is the frequency of the imposed motion and A_x its amplitude.

Six different sinusoidal motions have been imposed for each wind condition, the first six are in the below rated state, the second six approximately in the rated condition and the final six in the above one.

The aim of the tests was to study the response of the turbine to the simplest motion similar to the one encountered by a floating system. The low frequency displacements simulate the platform motion while the high frequency ones simulate the wave motion.

The thrust and the rotor torque have been measured and compared to the wind tunnel and FAST results in terms of mean value and amplitude variation.

As said previously all the simulations have been carried out both in wind and no-wind condition to eliminate the inertial component of the forces.

The procedure used for extrapolating the desired force data from the tests (figure ??) is the same used for the wind tunnel results, and can be summarized as follows:

- realignment of the two time series (wind and no-wind) based on the motion frequency band-pass filtered surge motion by detecting the zero crossing points
- detection of the displacement fundamental harmonic contribution from the force signals:

- implementation of the Fast Fourier Transform
- detection of the exact peak in the frequency domain
- reconstruction of the time domain fundamental force signal through Inverse Fourier Transformation
- computation of the aerodynamic force $F_{Aero} = F_{Tot} - F_{Inertial}$

	U [m/s]	Ω [rpm]	pitch angle [deg]	F_x [Hz]	A_x [m]
1				0.25	0.065
2				0.25	0.100
3	2.33	150	0.00	1.00	0.015
4				1.00	0.030
5				2.00	0.010
6				2.00	0.015
7				0.25	0.065
8				0.25	0.100
9	3.67	221	0.00	1.00	0.015
10				1.00	0.030
11				2.00	0.010
12				2.00	0.015
13				0.25	0.065
14				0.25	0.100
15	5.33	240	12.50	1.00	0.015
16				1.00	0.030
17				2.00	0.010
18				2.00	0.015

Table 4.5: Settings of the different simulations made for the unsteady analysis

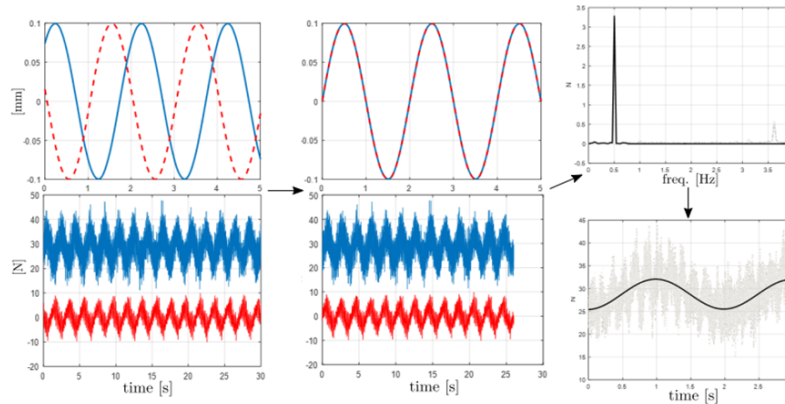


Figure 4.8: Flowchart for the data process leading to the detection of the aerodynamic force only from the imposed motion tests [7]

The analysis of the thrust results is shown in figure 4.9.

On the left-hand side, the comparison of the mean values, obtained by experimental tests in the wind tunnel and by numerical simulations in AdWiMo and FAST environments, shows an excellent agreement, as already underlined in the steady analysis.

On the contrary, the amplitude variation, on the right-hand side, is quite different between the wind tunnel results and the numerical simulations, in which it is lower. The good agreement between FAST and AdWiMo results has been expected, because the aerodynamic forces are calculated in the same way for the two software.

In figure 4.10 the same analysis made for the thrust is shown for the rotor torque.

In this case the results are worse, both in terms of mean value and in terms of amplitude variation. On the other way the two numerical software are consistent in the error.

This discrepancy can be explained in different ways but it is still under study.

First of all, the scaling design made for the Polimi turbine had, as its main objective, to match the real target thrust value instead of the target torque one.

Furthermore, the difference is to be attributed to the design and the calcu-

lation of the aerodynamic loads made by FAST module AeroDyn, used by both software, and not to the structural modeling or to the measure of the torque made by AdWiMo.

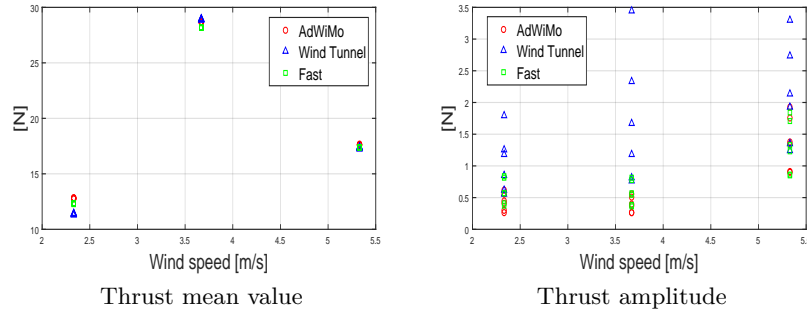


Figure 4.9: Thrust analysis for unsteady tests: comparison between numerical results (AdWiMo and FAST) and experimental ones

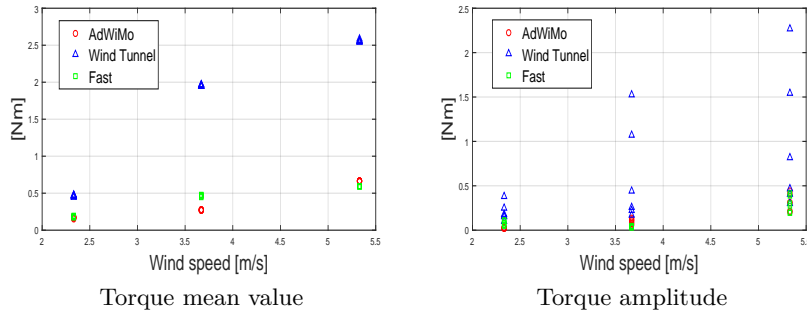


Figure 4.10: Torque analysis for unsteady tests: comparison between numerical results (AdWiMo and FAST) and experimental ones

A more in deep analysis of the thrust results has been made, both because it is the main target under study and because it is fundamental for the implementation of the 2-DoF wave model that will be presented in the next Chapter.

For each simulation the hysteresis cycle is obtained, plotting the measured thrust time series against the relative speed, calculated as the difference between the wind velocity and the one of the imposed motion.

The cycles obtained with AdWiMo simulations are compared to the ones obtained with the experimental campaign in the wind tunnel and with the simulations made in FAST environment (figure 4.11).

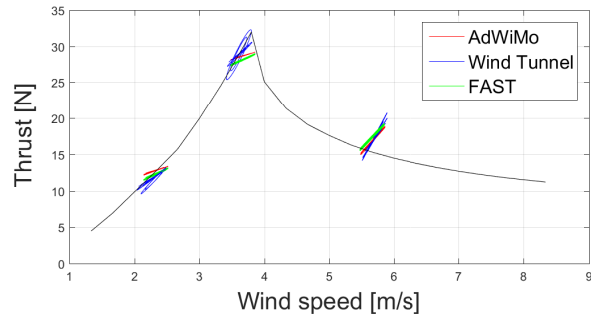


Figure 4.11: Hysteresis cycles obtained from the unsteady tests: comparison between experimental and numerical results

The behaviour is similar between the experimental and the numerical results, and practically identical between the FAST and the AdWiMo simulations.

Although the comparison of the thrust mean value is the same for all the three wind conditions, the slope of the hysteresis cycles between the wind tunnel tests and the simulations is different, especially for the rated condition.

Taking into consideration that the slope of the thrust hysteresis cycle can be described as an aerodynamic damping coefficient, while the minor axis of the ellipse indicates the aerodynamic added mass, some considerations about the results can be made:

- for the above rated wind condition the cycles are similar both considering the slope and the minor axis for both numerical and experimental tests;
- for the below rated condition some differences, especially in term of slope, can be seen between the wind tunnel and the simulation results;
- the rated wind condition is the most critical one because there are high differences about both slope and length of the minor axis of the ellipses;

- the wind tunnel hysteresis cycles, especially for the rated condition, are function of the frequency of the imposed motion, in fact different types of ellipses can be seen in the same wind condition. This peculiarity is not described by AdWiMo or FAST, for which the hysteresis cycle are coincident for all the simulations made at the same wind speed.

Chapter 5

Hydrodynamic model

As a result of the validation of the AdWiMo wind turbine model, the implementation of the hydrodynamic model will be presented in this Chapter. In Chapter 4, the tests carried out and the analysis made have underlined a good agreement between the numerical model and the target parameters, both numerical and experimental, in terms of thrust force, which is fundamental for the calculation of the sea state.

The differences that have been encountered in the previous analysis, especially in the unsteady simulations, must be taken into consideration for the evaluation of the future results.

First of all, the numerical model [1] that describes the sea state and the hydrodynamic forces will be briefly presented.

Then the experimental setup, used for the tests made in the wind tunnel, will be introduced, highlighting the methodologies used to overcome the scaling issues.

For this reason, an innovative real time hybrid (HIL) experimental approach has been utilized. This is helpful in exploiting separately the advantages of the wind-or-wave-only experiments, made in wind tunnel or in ocean basin, and mostly in passing the impossibility to keep, respectively, the Froude and Reynolds similitude between full and model scale, when testing a system subjected to the combined effect of gravity dependant loads (waves) and aerodynamic forces.

Therefore, the same numerical wave model used for the experimental tests in the wind tunnel has been linked with the AdWiMo wind turbine-robot model, taking advantage of the possibility of the Simulink co-simulation.

The design of the final rig will be explained, trying to make it as identical as possible to the real experimental setup.

Finally the results of the simulations will be presented, comparing them to the ones obtained by the wind tunnel tests campaign.

The simulations performed were of three type: the free decay tests, analyzing how the system returns to its equilibrium position after an imposed displacement, the regular wave tests and the irregular wave ones.

5.1 Hydrodynamic Numerical Model

The wave model has been developed considering only the two main degrees of freedom of the floating system: the *surge*, that is the displacement along the wind direction, and the *pitch*, that is the rotation to which the turbine is subjected due to the wind.

If the hypothesis of linearity is valid, the problem can be divided into three simpler problems: one for the radiation effect, one for the diffraction effects and one for the hydrostatic.

In reality a more complete model has to consider the non linear forcing introduced by the viscosity and the mooring.

In this section all the force components acting on the model will be briefly presented and then the final dynamic system, but before the wave theory will be introduced.

Surface Wave Theory

The wave motion causes a periodic loading on all the immersed structures in the sea.

Both wind and waves are irregular effects, and so they can be observed like an overlay of multiple components, each one with a proper amplitude, wavelength, frequency and direction.

In order to analyze the complete wave motion, it is important to know the property of each single regular wave of which it is composed.

In figure 5.1 the regular wave motion is presented in two different ways: on the left-hand side the wave is function of the distance x , while on the right-hand side the time history of a single water particle is shown.

The origin of the system is fixed on the sea level in a no-waves condition, with the z axes positive upwards.

The depth of the sea bottom h is measured with respect to the undisturbed

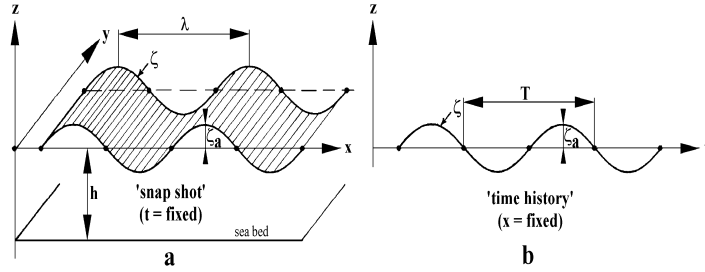


Figure 5.1: Regular waves

sea level.

The height of the wave can be described by a sinusoidal function with amplitude, equals to ζ_a , measured from the undisturbed sea level. The total height H is the peak-to-peak distance of the sinusoidal function :

$$H = 2\zeta_a \quad [m] \quad (5.1)$$

The distance between two wave peaks, measured along the horizontal axis, has two different meanings for the two different ways of describing the wave. In the "snapshot" plot it represents the wavelength λ , while in the "time history" plot it indicates the wave period T .

The last two parameters that describes the characteristics of a regular wave are the wave number k and the angular frequency ω , defined as:

$$k = \frac{2\pi}{\lambda} \quad \left[\frac{rad}{m} \right] \quad (5.2)$$

$$\omega = \frac{2\pi}{T} \quad \left[\frac{rad}{s} \right] \quad (5.3)$$

Finally the equation of the wave profile along the x direction can be expressed, both in function of x and time, in the following way:

$$\zeta = \zeta_a \cos(kx - \omega t) \quad (5.4)$$

The regular waves theory, known as Airy's linear theory, is based on the potential flow and can be applied only assuming that the slope of the wave is low.

In figure 5.2 the validity zones of the different wave theories are indicated, on the horizontal axis the adimensional depth $\frac{h}{gT^2}$ is represented while on

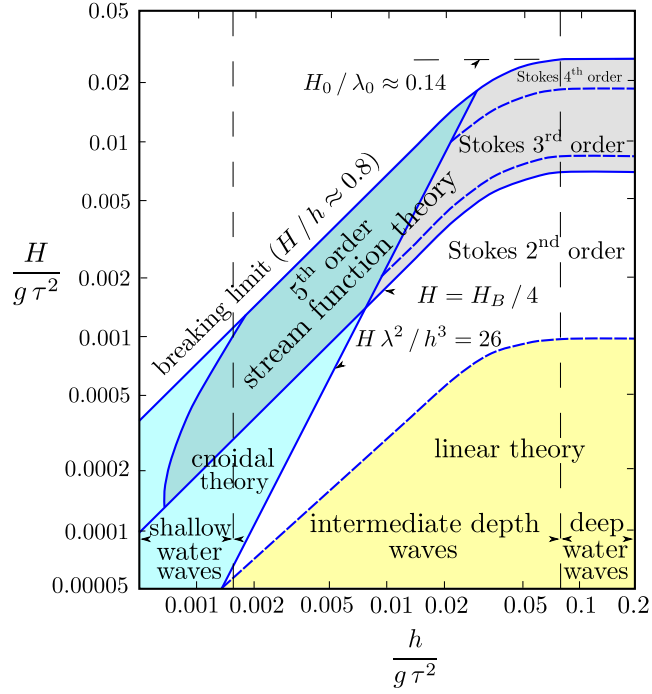


Figure 5.2: Validity of the different wave theories

the vertical one the adimensional slope $\frac{H}{gT^2}$.

The yellow zone is the range of validity of the Airy's linear theory, it is valid for high depths, where the floating offshore wind turbine are generally installed, and for a large interval of different wave heights.

Exploiting the regular waves theory and the superimposition principle a more detailed model can be developed, introducing the irregular wave theories as the sum of different regular waves.

There are numerous representations of the irregular sea state in literature, like the JONSWAP or the white noise.

The irregular waves model obtained from the Airy's theory does not described correctly a series of low frequency harmonics. A greater degree approximation is needed, introducing the so-called second order irregular wave, which are the one used for the wind tunnel simulations.

5.1.1 Time domain numerical model

In this section the time domain numerical model will be presented. Besides the 2 DoF hypothesis, another assumption has been taken in order to simplify the model complexity: the entire wind turbine has been considered as a rigid body, so as the inertial forced related to it can be calculated in a simple way, neglecting the aero-elastic effects of the tower and the blades.

The final hydro-aero-elastic model can be consider as a mass-damper-spring mechanical system subjected to different forces. Every physical effects acting on the turbine or on the floating platform contribute to the final equation of motion, and they are separately analyzed afterwards.

The equation 5.5 represents the final mechanical system that describes the floating offshore wind turbine subjected to wave and aero forcing. The \underline{x} vector contains the two independent coordinates for surge and pitch motions, as $\underline{x} = [x, \vartheta]^T$. On the left-hand side the following 2x2 system matrices can be recognized: $[M_s]$ is the structural mass, $[A_\infty]$ is the "infinite frequency" hydrodynamic added mass matrix due to the radiation of the submersible platform, $[R_s]$ is the diagonal viscous linear damping matrix and $[K_s]$ is the system stiffness matrix containing both the terms related to the hydrostatic as well as the gravitation effect.

On the right-hand side the force vectors of different types are summed to provide the effective motion to the system [4].

$$\begin{aligned} & [[M_s] + [A_\infty]]\ddot{\underline{x}} + [R_s]\dot{\underline{x}} + [K_s]\underline{x} = \\ & = F_{moor} + F_{diff}^{(1)} + F_{diff}^{(2)} + F_{rad} + F_{visc} + F_{aero} \end{aligned} \quad (5.5)$$

Inertial matrix

The matrix of inertia is obtained from the first derivative of the kinetic energy through the Lagrange method. It can be considered constant under the hypothesis of small displacements.

In figure 5.3 the complete floating system can be seen. The mass properties, the centers of mass of the bodies and their distances compared to the sea level are shown and have to be used for the formulation of the mass matrix.

$$[M_s] = \begin{bmatrix} M_{tot} & S \\ S & J_{tot} + J_{tr} \end{bmatrix} \quad (5.6)$$

Where:

- $M_{tot} = m_{pl} + m_{to} + m_{na} + m_{ro}$

- $J_{tot} = J_{pl} + J_{to}$
- $S = m_{pl}Z_{pl} + m_{to}Z_{to} + (m_{na} + m_{ro})Z_{na}$
- $J_{tr} = m_{pl}Z_{pl}^2 + m_{to}Z_{to}^2 + (m_{na} + m_{ro})Z_{na}^2$

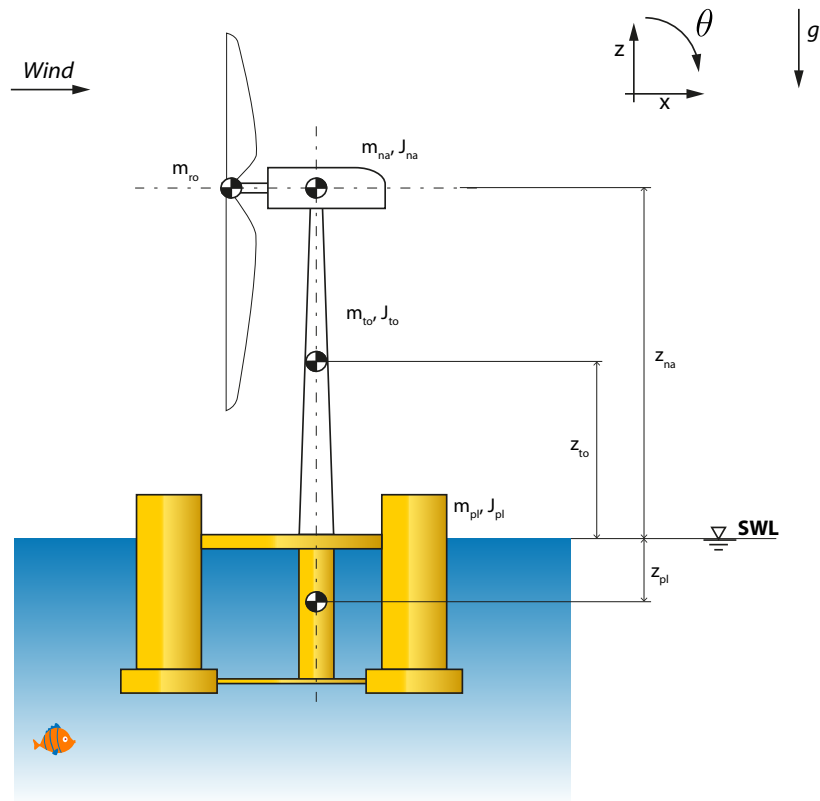


Figure 5.3: Scheme of the complete system

Stiffness matrix

The stiffness matrix is composed by two elements: the hydrostatic component and the gravitational one.

The first is in turn composed by two terms: the Archimedes force, from which depends the static position of the system, and the straightening force, which guarantees that the system returns to its equilibrium position after a

perturbation.

The gravitational component can be calculated linearizing the gravitational potential energy around the equilibrium position.

Radiation force

The radiation force describes the dissipation of energy of the platform motion due to the radiated waves generated by the platform itself.

It is partially accounted by the term $[A_\infty]$ and it is calculated as the convolution between the platform velocity \dot{x} and the impulse retardation function. Due to the time consuming computation of a convolution term for a real-time application, the force is firstly calculated in the frequency domain.

Viscous force

The viscous forces considered are due to the Morrison's contribution, derived by the integration along the three semi-submersible pontoons of the drag forces, depending quadratically on the relative velocities between the platform and the wave particles, either along the tangential and the axial direction.

The forces are firstly calculated in the local reference frame of each pontoon, and then transposed to the global one coherent with the wind turbine.

The tests made in the ocean basin at MARIN (Maritime Research Institute Netherlands) have highlighted the need to introduce into the numerical model a linear damping contribution that is not modeled in the theoretical formulation of viscous forces.

The damping matrix is then formulated as follows:

$$[R_s] = \begin{bmatrix} 45000 & 0 \\ 0 & 1 \cdot 10^8 \end{bmatrix} \quad (5.7)$$

Mooring lines force

The system is anchored to the sea bottom through a complex system of mooring. In the studied case it is composed by three chains connected to the pontoons with a 120 deg angle offset.

The non-linear elastic forces were obtained computing the static loads using FAST coupled with the MoorDyn module, by imposing a set of displacements so as to generate two interpolating surfaces (one for the surge and

one for the pitch) to be used as look-up tables during the experiments.

First order diffraction force

The linear diffraction forces are related to the waves generated externally to the floating structure. They are obtained based on complex frequency dependant wave exciting force vector and for a unitary wave amplitude, for each degree of freedom, under the assumption of a linear wave surface approximation.

They are computed considering the random phased wave amplitudes JON-SWAP spectrum.

Second order diffraction force

The second order diffraction forces are needed in order to have a more accurate approximation of the wave motion with respect to the linear ones.

They derive from the combined effect of pairs of incident waves at different frequency on the structure. Although these forces are not comparable, in absolute value, to the linear ones, their effects are relevant because they can excite in resonance the rigid modes of the floating system.

Aerodynamic force

The aerodynamic forces are the ones measured at the hub of the wind turbine, properly purified from the inertial contribution.

Under the hypothesis of rigid wind turbine, the reaction forces at the tower base are equal to the aerodynamic ones, and can be easily measured.

5.2 Experimental setup and implementation

The complete dynamic equation, designed in the previous section, can be solved in real time by a Simulink model that calculates the vector forces and integrates the equation of motion.

This is useful to implement an hybrid numerical-experimental approach, called Hardware-In-The-Loop (HIL), for the study of the full system in the

wind tunnel. It consists in a real-time computation of the equation of motion, using the Simulink model, together with the direct measure of the aerodynamic forces acting on the wind turbine.

The HIL method allows to simulate directly complex sea states, such as the irregular conditions, and evaluating the combined effect of hydrodynamic and aero-elastic forces.

In this section the experimental setup and its implementation will be presented, focusing on the physical system tested in the wind tunnel, and on the method used to correctly calculate the aerodynamic forces, eliminating the inertial loads instant per instant.

5.2.1 Real model

The real model tested in the wind tunnel at Politecnico di Milano is shown in figure 5.4. It is composed by the scaled wind turbine described in the previous chapters, a platform that is able to repeat the 2 DoF movement of the floating system and the measuring equipment.

The platform will be substituted by the hexapod robot when a 6 DoF sea state will be tested.

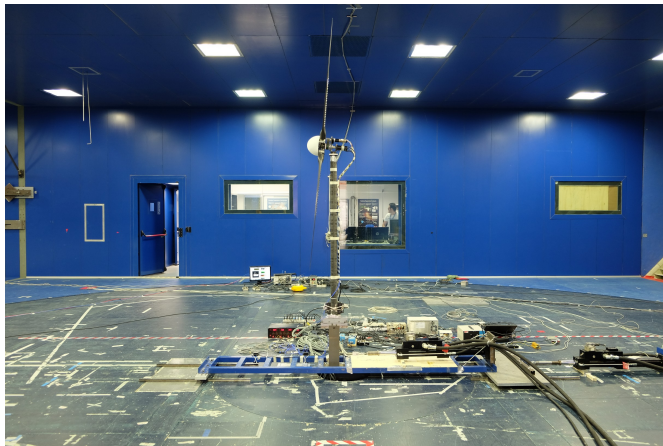


Figure 5.4: Real model used for wind tunnel tests

The handling mechanism consists in a long cart that runs on the guides fixed to the ground. The horizontal displacement, equivalent to the surge degree of freedom, is generated through an hydraulic actuator connected to

the bogie on one side and to the ground on the other. Another actuator is placed on the cart and generates the pitch rotation using a crank mechanism. The kinematic system is outlined in figure 5.5, because the force measures are obtained at the same level of the water, the two degrees of freedom of the system are calculated inverting the following kinematic relationship:

$$\begin{pmatrix} act_1 \\ act_3 \end{pmatrix} = \begin{bmatrix} 1 & -\frac{b_1}{b_2} \\ 0 & -\frac{1}{b_2} \end{bmatrix} \begin{pmatrix} x \\ \vartheta \end{pmatrix} \quad (5.8)$$

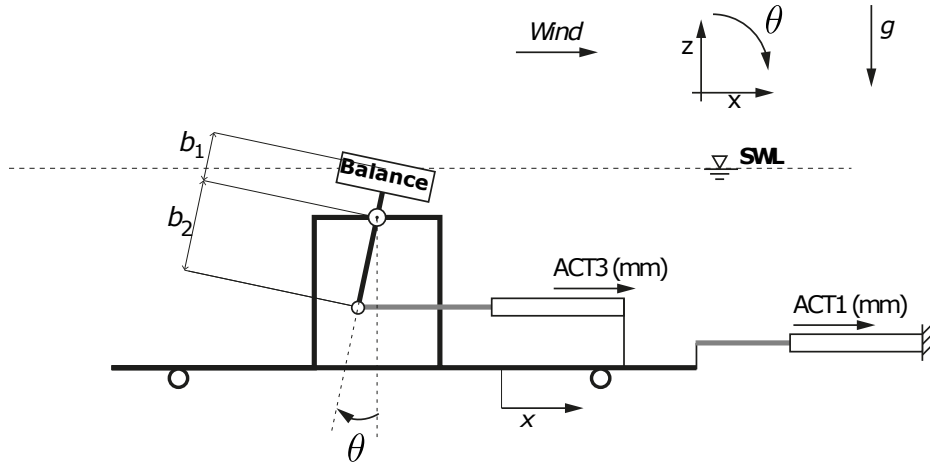


Figure 5.5: 2 Dof platform kinematic

Two precision balances are used to measure the aerodynamic forces: one is collocated at the base of the tower of the wind turbine, it is a typical measuring instrument used in the wind tunnel and it is called RUAG. The other is placed in the nacelle zone and it is called ATI. Both of them are able to measure six force components, one for each axis and the three related torques.

About the wind turbine, the tower and the three blades are made of carbon fiber, in order to match the requirements needed for a correct stiffness scaling. The hub is composed by two carbon plates that contain the actuators used for the control of the pitch angle of the blades.

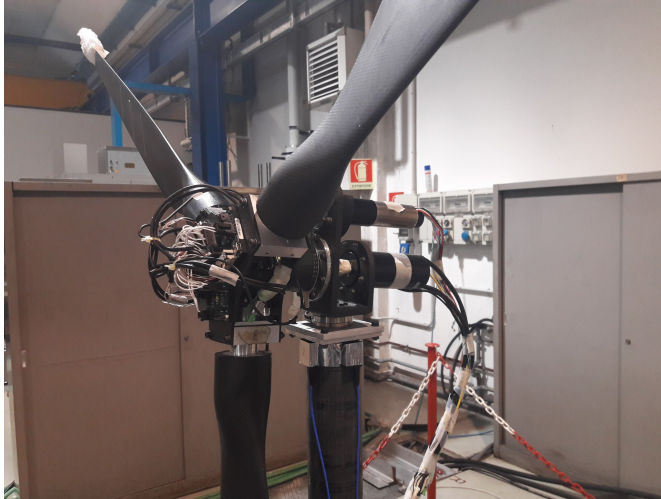


Figure 5.6: Polimi wind turbine rotor and nacelle

5.2.2 Control and actuation model

In this section the control logic and the actuating system used for simulating the floating platform movement will be presented.

At first the measuring instrumentation will be shown, focusing on the critical aspects, and then the measured force correction will be described. This correction is necessary because the inertial parameters of the scaled model are not perfectly the ones of the full-scale turbine, because of the instrumentation and other mechanical requirements.

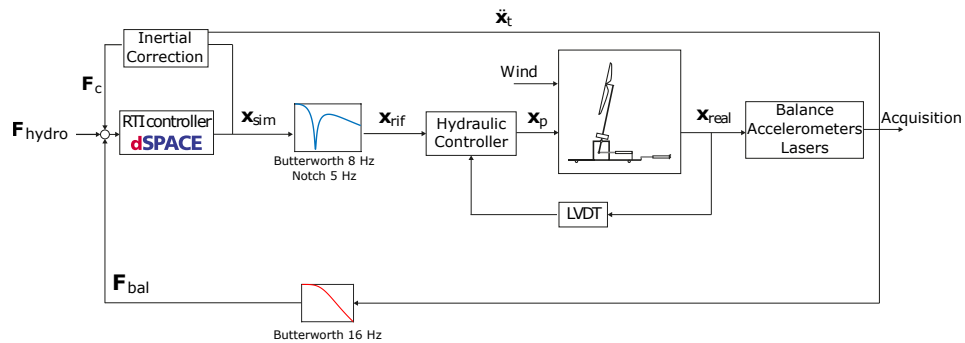


Figure 5.7: Wind tunnel control logic

In figure 5.7 the control logic used for the wind tunnel test is schematized. It is constituted by a real time controller (*RTI controller dSPACE*) that solves the equation of motion (5.5) in function of the sum of the forces F_{hydro} , F_{bal} and F_c . The first one is the sum of all the forces related to the hydrodynamic effects, while the second and the third represent the aerodynamic force (they will better explained later). The balance force is filtered with a second order low-pass Butterworth filter with a cut-off frequency of 16 Hz.

The obtained numerical state vector \underline{x}_{sim} is then filtered with a low-pass second order Butterworth filter (cut-off frequency equals to 8 Hz) and with a notch filter at 6.5 Hz, used to remove the frequency components equals to the first mode of vibration of the system, in order to limit the resonance effects.

The filtered signal \underline{x}_{rif} becomes the reference for the hydraulic control loop, that controls the position of the hydraulic actuators through *LVDT* (Linear Variable Displacement Transducer) position sensor.

In addition, the measurement system is composed by: the two six-components balances (the RUAG placed at the tower base, the ATI placed between the tower and the nacelle), MEMS accelerometers positioned along the tower and laser position meters.

The measurement chain, the actuation of the pistons and the filters introduce a series of delays among the different signals, causing a time shift between the numerical simulation and the measured force, whose effect is an additional damping on the overall system.

These delays has been estimated through a series of imposed motion tests for both the actuators, obtaining two transfer functions to be applied on the control loop.

Correction of the measured force

The wind tunnel model is not perfectly scaled in terms of mass and stiffness due to the presence of the measuring equipment. For this reason, the measured forces, that are composed of a part due to aerodynamics and one due to the inertia of the physical model, do not represent the expected loads.

With reference to the figure 5.8, for a generic (positive) state of the motion variables x and ϑ , the forces measured by the RUAG balance, placed between the wind turbine model and the motion mechanism, are due to inertia, gravitational stiffness and aerodynamic forces, as written in the equation 5.9

$$F_{bal} = - \begin{bmatrix} m_t & b_t m_t \\ b_t m_t & b_t^2 m_t + J_t \end{bmatrix} \ddot{x}_t + \begin{bmatrix} 0 & m_t g \\ 0 & m_t b_t g \end{bmatrix} x_t + F_{aero} \quad (5.9)$$

where mass, momentum of inertia and center-of-mass position of the wind turbine, indicated with the subscript t , have been experimentally derived by means of imposed motion tests. Furthermore, the surge force measured by the balance, F_{bal} , is assumed to be along x even if it is in the balance's rotating reference frame, considering small ϑ angles for the linearization.

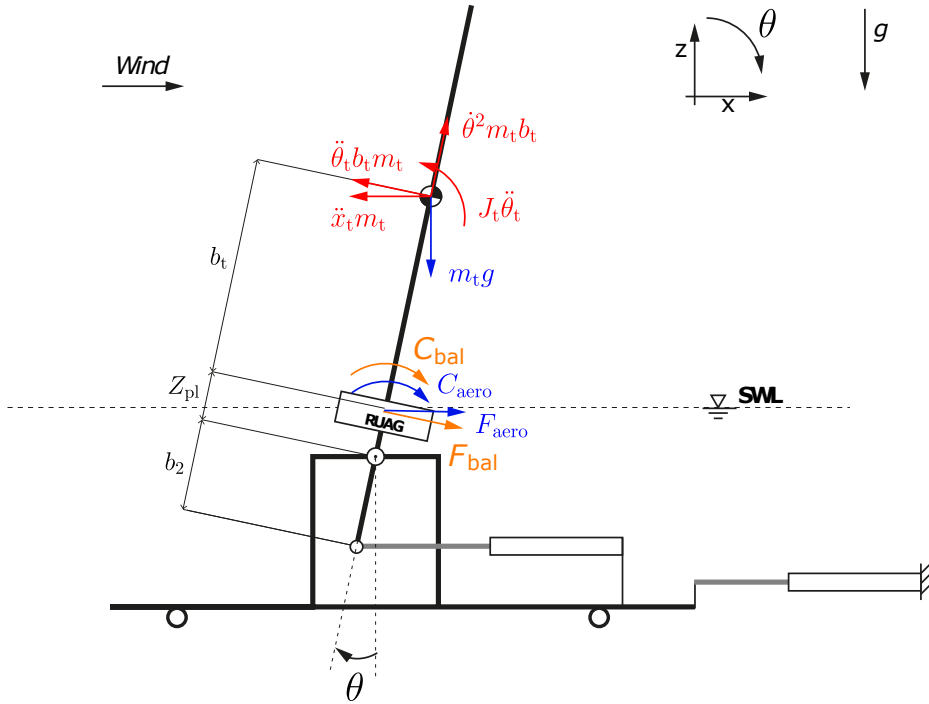


Figure 5.8: Forces acting on the physical system

If the mass and the momentum of inertia of the wind turbine perfectly matched the model scaling requirements, the equation 5.5 could be modified as follows:

$$[[M_{pl}] + [A_{\infty}]] \ddot{x} + [R_s] \dot{x} + [K_{pl}] x = F_{hydro} + F_{aero} = F_{hydro} + F_{bal} + F_c \quad (5.10)$$

where the subscript *pl* stands for "platform", indicating that on the left-hand side only the platform terms are considered while the wind turbine inertial and gravitational terms are measured on the right-hand side by the vector F_{bal} , with only a single term correction vector F_c :

$$F_c = \begin{bmatrix} 0 & -m_t g \\ 0 & 0 \end{bmatrix} \underline{x}_t \quad (5.11)$$

Knowing that a perfect scaled model is hardly reachable, the equation of motion 5.5 has to keep the whole system matrices, and became:

$$[[M_s] + [A_\infty]]\ddot{\underline{x}} + [R_s]\dot{\underline{x}} + [K_s]\underline{x} = F_{hydro} + F_{aero} = F_{hydro} + F_{bal} + F_c \quad (5.12)$$

with the term F_c which eliminates all the inertial and gravitational terms. The correction term requires the exact knowledge of the system state, which turned out to be troublesome. Therefore the effective wind turbine state was assumed to be equal to the simulated one.

The aerodynamic forced used for the HIL approach are then the following one:

$$\begin{aligned} F_{aero} &= F_{bal} + F_c = \\ &= F_{bal} + \begin{bmatrix} m_t & b_t m_t \\ b_t m_t & b_t^2 m_t + J_t \end{bmatrix} \ddot{\underline{x}}_{sim} + \begin{bmatrix} 0 & -m_t g \\ 0 & -m_t b_t g \end{bmatrix} \underline{x}_{sim} \end{aligned} \quad (5.13)$$

5.3 AdWiMo-Simulink HIL model

In this section the creation of the final integrated numerical test rig will be presented. The model has to represent faithfully the wind tunnel experiments on floating offshore wind turbines made at Politecnico di Milano, using the same correction of the forces explained in the previous section.

The model uses the same HIL approach explained in the figure 5.7, but with the real experimental setup (wind turbine and moving cart) substituted by the Simulink block representing the AdWiMo numerical model (wind turbine and hexapod robot). For this reason the numerical test rig is not properly an Hardware-In-The-Loop system but, more precisely, a Software-In-The-Loop control logic, where the equation of motion and the hydrodynamic forces are integrated and calculated in the same way as in the real wind tunnel tests, while the F_{bal} and the F_c components, used for computing the real

aerodynamic force, are measured inside the AdWiMo environment. The numerical rig has been used to replicate the same tests carried out in the wind tunnel on the 2-DoF system in order to verify its correctness, and it will be of great importance for the future implementation of the 6-DoF hydrodynamical model, in fact it will be a prediction tool to be used before testing the expensive real wind turbine-robot system. For this reasons, every aspects of the real model has been studied and replicated where possible. A more in deep analysis of the communicating time interval and sampling frequencies of all the measurement tools and real time controller have to be made in order to have a perfect dual model.

The AdWiMo system is added to the hydrodynamic model through the co-simulation approach explained in Chapter 3. The wind turbine and the hexapod robot are then schematized like a simple Simulink block with the desired inputs and outputs.

All the wind turbine bodies and the robot sliders are set as rigid parts in order to neglect the aero-elastic effects, especially of the tower and the blades. The selected dynamic solver in the AdWiMo environment is the GSTIFF, with an integration error of 0.01. The integrated time step is set to 0.005 s, this choice is due to the need to have the same time interval in the two numerical environment, Matlab and Adams, in order to get a correct co-simulation. Furthermore it is the same time step as the one used to define the wave time series and the hydrodynamic forces.

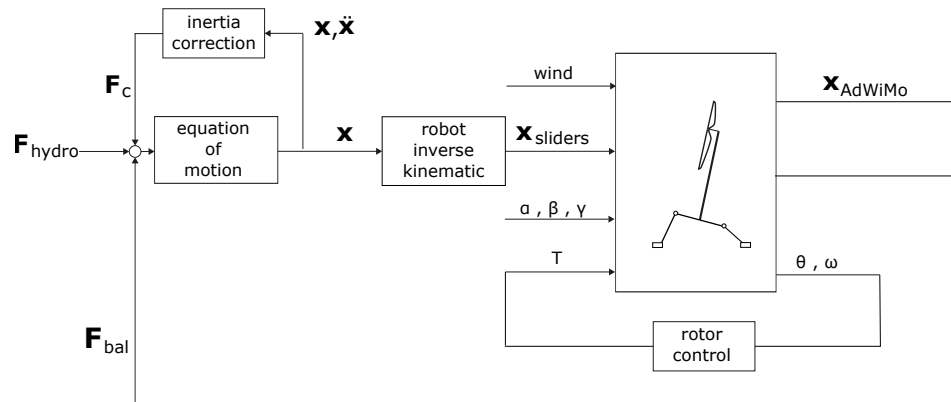


Figure 5.9: AdWiMo-Simulink HIL control logic

In figure 5.9 the final test rig made by the co-simulation between Ad-

WiMo e Simulink is presented. The aerodynamic forces, previously measured directly in the wind tunnel, are now numerically calculated in the AdWiMo environment using the same correction of the inertia of the experimental case. The hydrodynamic effects that in the real case are computed by a real-time controller are now calculated by a Simulink model that solve the equation of motion as described in the section 5.1.1.

As shown in figure 5.9, the AdWiMo block is composed by the scaled wind turbine and the hexapod robot system. The wind, and then the aerodynamic forces, comes from the FAST subroutine like in a normal AdWiMo simulation.

The inputs of the block are the six motion of the robot sliders, the three blade pitch angles and the rotor control torque. The six motions are obtained through a kinematic inversion of the two degrees of freedom, the surge and the pitch, calculated solving the dynamic equation of motion of the floating platform. They are defined as velocities and not as displacements in order to maintain the continuity with the previous imposed motion simulations made for validating the software (see section 4.3), despite actually the problem related to the acceleration discontinuity is no longer presents (there is no more the necessity to define the motion through a cubic spline interpolation of the time series).

The α , β and γ are the blade pitch angles, they are defined by the user, before the beginning of a simulation, as constant and they are function of the wind condition that the user want to test.

The rotor torque is calculated by a closed control loop enclosed inside the AdWiMo block. The control logic is the same shown in figure 3.8. As said previously in Chapter 3, the reference rotor speed is obtained with a short transient time and without steady state error, the negative effect is a very high torque that move the system from its equilibrium position, it will therefore be necessary to wait some seconds in order to let the system returns to its equilibrium point.

The outputs of the AdWiMo block are the motion of the platform (i.e. the base of the tower), the angular displacement and the speed of the rotor and the reaction forces obtained at the base of the tower.

The platform motion is equivalent to the one made by the wind turbine, it is collected inside the vector \underline{x}_{AdWiMo} containing the surge and the pitch degrees of freedom of the system, and it will compared to the equivalent vector obtained in the wind tunnel experimental test in order to verify the correctness of the numerical rig.

The rotor displacement and speed are used to close the rotor control loop. They are measured directly in the AdWiMo environment with properly unit

of measure.

The reaction forces represents the F_{bal} used in the real experimental loop, they are equivalent to the forces measured by the RUAG balance. In the numerical system they are a 2x1 vector, that contains the force along the wind direction and the torque relative to the pitch degree of freedom, measured at the fixed joint that connects the tower to the robot platform. The forces are related to a moving marker placed in the same position of the constrain and in agreement with the platform motion. In this way the measure is coherent with the the RUAG one, see figure 5.8.

The aerodynamic forces are then completed with the vector F_c (equation 5.13) computed with the correction of the inertia method previously explained. The state vector \underline{x} and its second derivative $\underline{\ddot{x}}$ are the ones obtained integrating the equation of motion. The mass, the momentum of inertia and the height of the center of gravity, needed for calculating the matrices, are obtained with the AdWiMo mass tool and they are equal to the ones shown in table 3.10, except for the momentum, because the equation needs the one referred to the center of mass of the system. It is calculated in this way:

$$J_t = I_{yy} - m_t \cdot b_t^2 = 1.005 \text{ Kg}m^2 \quad (5.14)$$

The final numerical model is then completed with the same filters, and with the delays related to the actuators, that are present in the real HIL system, in order to have a test rig that is as close to reality as possible.

Before simulating the same tests made in the wind tunnel, some imposed sinusoidal motions, applied to both the degrees of freedom, and varying their amplitude and frequency, have been substituted to the real platform state calculated by the hydrodynamical equation of motion, in order to verify the correctness of the model.

All these simulations were made in a no wind condition, and then the sum of F_{bal} and F_c was calculated. If it is equivalent to the aerodynamic force F_{aero} , it has to be equals to zero for all the imposed motion simulations.

The tests showed a not null force, so the model was not correctly designed. The error was due to a time-shift of the two force components introduced by the filters and the delays.

So the complete numerical model does not foresee the use of the filters, while the time delays are imposed equal to the integration time step of the simulation. The same tests have shown a correct inertia correction this time.

The test rig is therefore not perfectly dual compared to the real experimental setup, but it works in the same correct way. In order to take into account the filters, the measurement and actuating system a more in deep analysis has to be made, especially of the delays that have to be introduced to the

numerical system.

5.4 Wind tunnel tests

In this section all the tests made in the wind tunnel and replicated with the numerical test rig will be presented and analyzed.

The aim of the comparison is to understand if, and how good, the AdWiMo model, coupled with the hydrodynamic formulation, is able to repeat the wind tunnel tests on floating offshore wind turbine, and then if it can be used as a support for the future implementation of the 6-DoF wave model. The tests are divided into three different categories: the decay tests, both on the surge and on the pitch degree of freedom, the regular waves and the irregular ones.

Depending on the type of test the user wants to simulate, the initialization procedure of the model is different. It can be summarized as follows:

- load the wave characteristics and the hydrodynamic forces in Matlab environment;
- load the AdWiMo system block in Matlab environment;
- if the simulation involves wind and aerodynamic forces, they are activated after 5 seconds, as the AdWiMo convention, and at the same time also the rotor control torque is imposed;
- if the test is a decay, after the rotor transitory:
 - activate an additional damping;
 - imposed the necessary force or torque in order to move the system from its equilibrium condition to the desired point;
 - remove the additional damping;
 - remove the force/torque.
- if it is a test with forcing waves , after the rotor transitory, enable the hydrodynamic forces.

5.4.1 Decay tests

The first tests made are the decay ones. They consist in the system let free to move after an initial displacement from its equilibrium position, without

any hydrodynamical force acting on it. The system is tested on both the degrees of freedom, with and without the wind. It is interesting to see that the introduction of the aerodynamic force changes a lot the response of the numerical system, but it is predictable analyzing the unsteady tests carried out on only the wind turbine in the AdWiMo environment (see section 4.3).

In figure 5.10 the decay tests imposed on the surge degree of freedom are presented. The system is moved of 100 mm from its equilibrium position and then let free to move. The tests are made in a no wind condition firstly, and then in three different conditions of the wind: below rated (3.1 m/s), rated (3.8 m/s) and above rated (4.67 m/s). The results show an excellent agreement between the wind tunnel tests and the AdWiMo simulation, especially for the no wind and the above rated conditions.

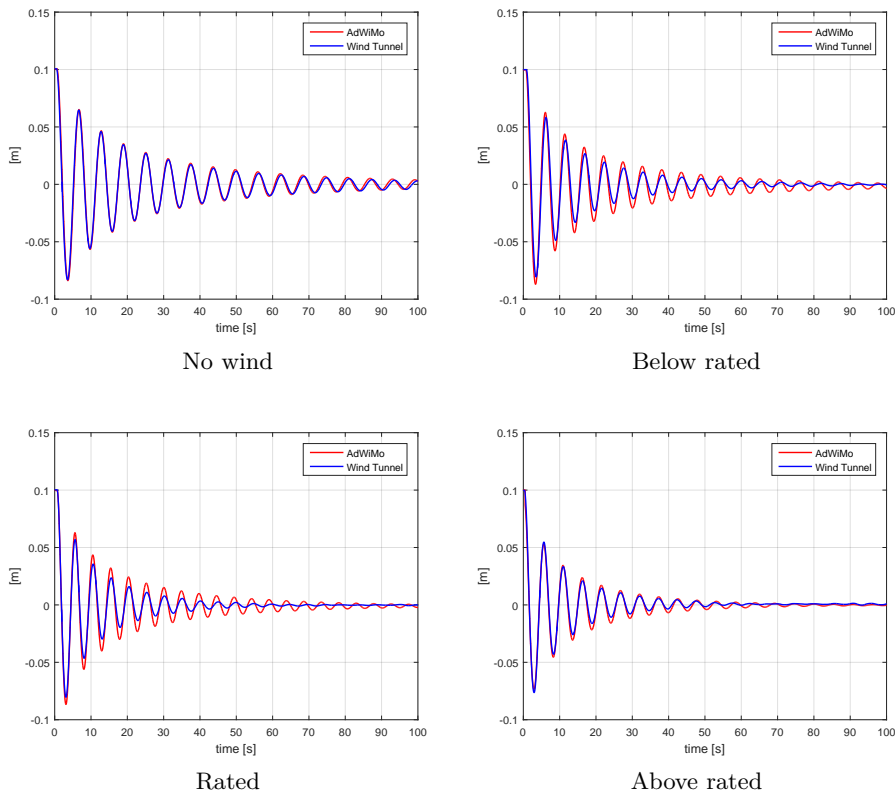


Figure 5.10: Surge decay tests for different wind conditions

Also the pitch degree of freedom is tested in a decay test. The system is moved of 8 deg from its equilibrium position and for all the wind conditions previously listed. This time the results, figure 5.11, show a good agreement in the no wind and above rated conditions, while for the below rated and the rated ones the simulations indicate a low level of damping compared to the real system.

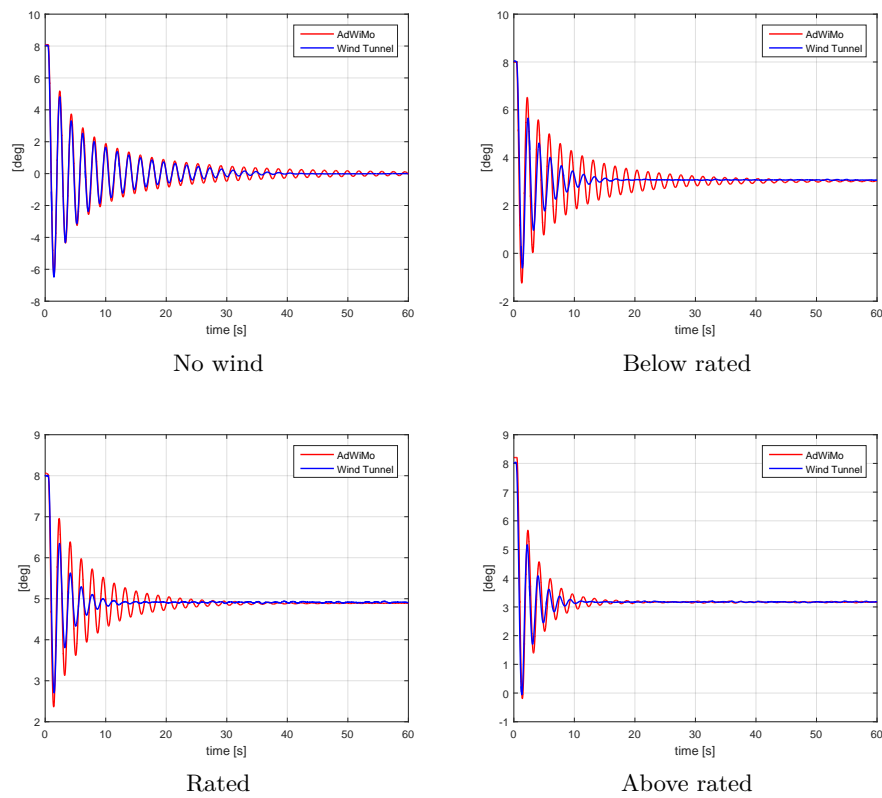


Figure 5.11: Pitch decay tests for different wind conditions

The disagreement in the below rated and in the rated conditions, and the difference response of the two degrees of freedom in the decay tests, can be explained observing the previous unsteady analysis made on the wind turbine and presented in the section 4.3.

In that case the hysteresis cycles, that are an indication of the added mass and damping due to the aerodynamic forces, are coincident, for the high

wind velocity condition, between the software and the wind tunnel. While for the below rated and, especially, for the rated conditions, their slope is very different between the numerical and the experimental results. This discrepancy is reflected in the decay tests.

The different behaviour of the two degrees of freedom (the surge is generally more coincident with the wind tunnel results than the pitch, also for the two critical wind conditions) can be explained always analyzing the hysteresis cycles. From figure 4.11, it can be noticed that the wind tunnel results are dependent on the frequency of the imposed motion; in fact, varying the frequencies, the slope of the cycles change, indicating a different level of added damping on the system.

In figure 5.12 the Fourier transform of the two degrees of freedom subjected to a decay test are shown, it can be seen that the proper frequency of the pitch is approximately three times higher than the one of the surge.

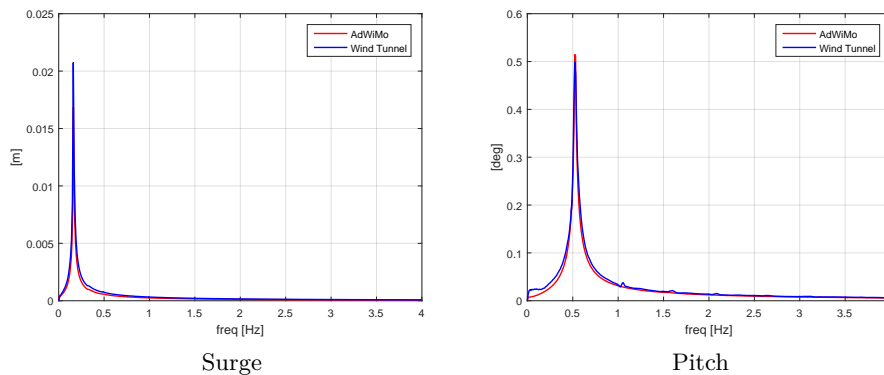


Figure 5.12: Fourier transform of the two degrees of freedom for the decay test

The no wind condition has been analyzed more in deep, comparing the results obtained with the numerical test rig with the ones obtained in the wind tunnel and also with the one obtained in the ocean basin at Marintek. In table 5.1 the proper frequencies of the two degrees of freedom are presented, showing an excellent agreement (the frequencies are expressed in the full scale dimension).

In table 5.2 the results of the damping analysis are shown. The analysis consists in a linearization of the decrease of the motion amplitude. Measuring the first i peaks of the decay plot, the following quantities have been

calculated:

$$\xi = \frac{\Phi_n - \Phi_{n+1}}{\frac{1}{2}(\Phi_n + \Phi_{n+1})} \quad (5.15)$$

$$\bar{\Phi} = \frac{1}{2}(\Phi_n + \Phi_{n+1}) \quad (5.16)$$

where Φ_n is the amplitude of the generic motion peak. The decrease of motion amplitude ξ is plotted against the average motion amplitude $\bar{\Phi}$, obtaining $i-1$ points that have to be interpolated through a straight line. The coefficients p and q in the table 5.2 are the intercept and the slope of the line, and they represent, respectively, an indication of the linear and the quadratic damping of the system.

	Surge [Hz]	Pitch [Hz]
AdWiMo	0.0091	0.0301
HIL	0.0091	0.0311
MARIN	0.0094	0.0308

Table 5.1: Proper frequencies of the two degrees of freedom

	Surge		Pitch	
	p	q	p	q
AdWiMo	0.134	0.069	0.101	0.053
HIL	0.107	0.075	0.150	0.051
MARIN	0.156	0.107	0.042	0.075

Table 5.2: Damping parameters for the two degrees of freedom

5.4.2 Regular wave tests

The system is also tested against the hydrodynamic motion. Firstly different types of regular waves are simulated, even if they are not a realistic condition.

The tests have been performed both in a no wind condition and in a rated one, knowing that the discrepancy due to the aerodynamic damping, showed in the previous section, will be attenuated by the hydrodynamic forces, that are greater in magnitude than the aerodynamic one.

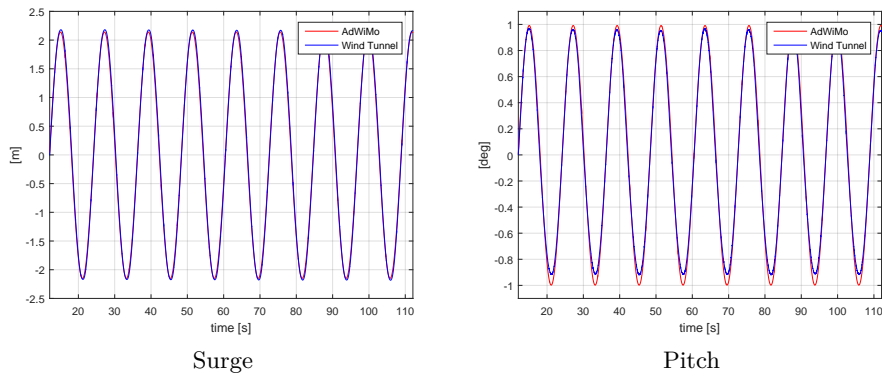


Figure 5.13: Regular wave test in no wind condition

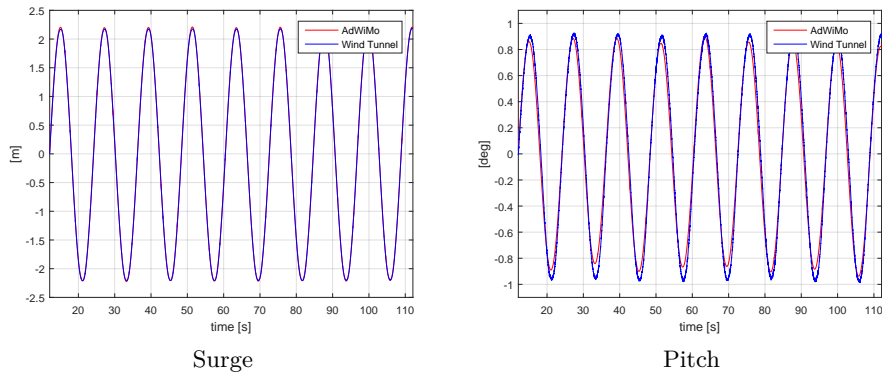


Figure 5.14: Regular wave test in rated wind condition

The results presented in the figure 5.13, for the no wind condition, and in the figure 5.14, for the rated one, show how the two degrees of freedom respond to a wave with height $H = 7.2 \text{ m}$ and period $T = 12.1 \text{ s}$. The comparison of the surge is practically perfect between the numerical tool and the wind tunnel both in term of amplitude and frequency. The pitch shows

a very good agreement between the two results, with a little discrepancy in amplitude.

5.4.3 Irregular wave tests

The last tests carried out are the ones where the system is subjected to an irregular wave. This is the operative condition more critical for the floating system because this is the case in which the forcing is present in all the spectrum of frequencies.

The results shown in the following figures (in model scale dimensions) are related to an irregular wave of the second order, with height $H = 7.2 \text{ m}$ and period $T = 12.1 \text{ s}$.

The figures 5.15 and 5.16 refer to the response of the two degrees of freedom in the no wind condition, while the figures 5.17 and 5.18 in the rated wind condition. Both the temporal domain and the PSD (power spectral density) are presented. The PSD permits an easier comparison between the numerical and the experimental results. Generally a good agreement can be seen for both the surge and the pitch in both wind conditions.

It is important to notice that there are components at low frequencies, that are between 0 and 1 Hz (0 and 0.05 Hz in full-scale dimensions). They are caused by the initial transitory of the simulations that coincide with the proper frequencies of the rigid motions of the system.

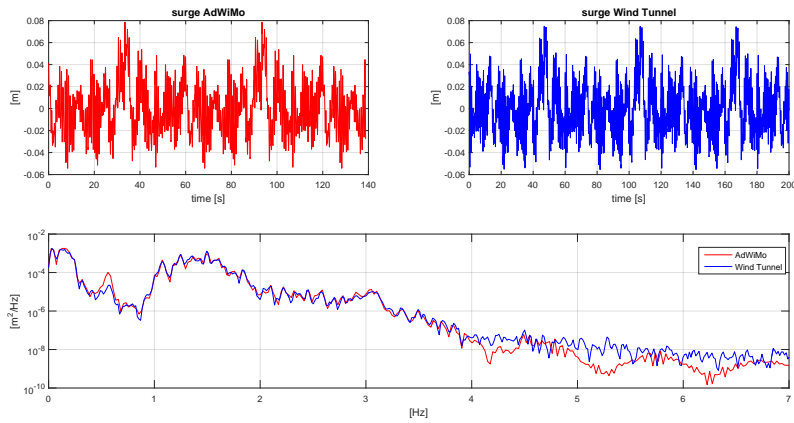


Figure 5.15: Surge result for the irregular wave test in no wind condition

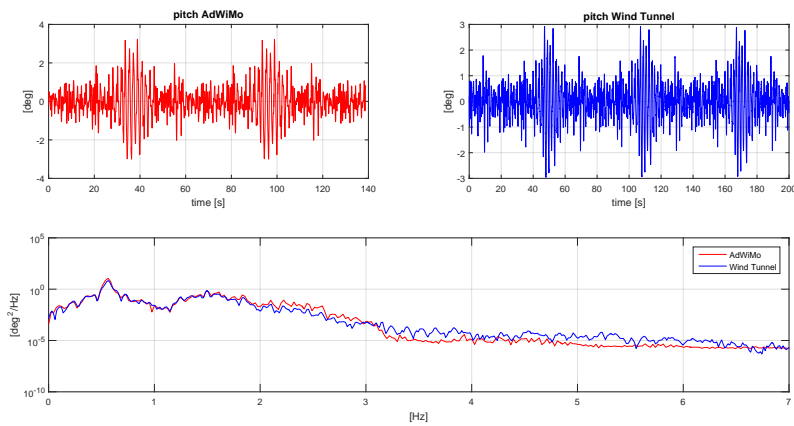


Figure 5.16: Pitch result for the irregular wave test in no wind condition

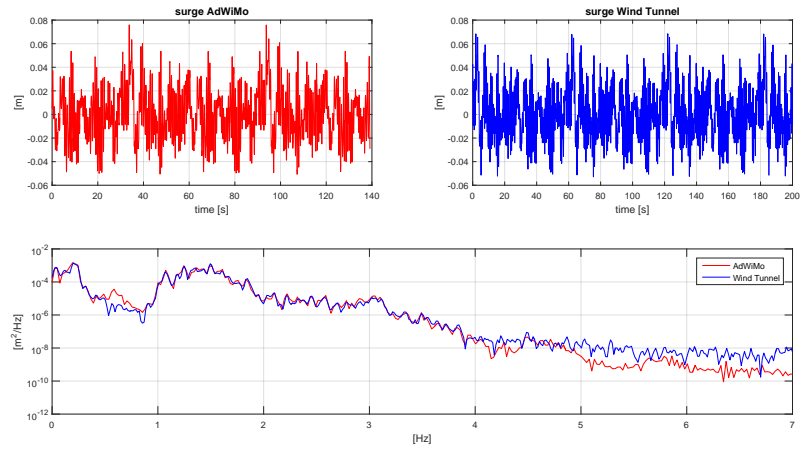


Figure 5.17: Surge result for the irregular wave test in rated wind condition

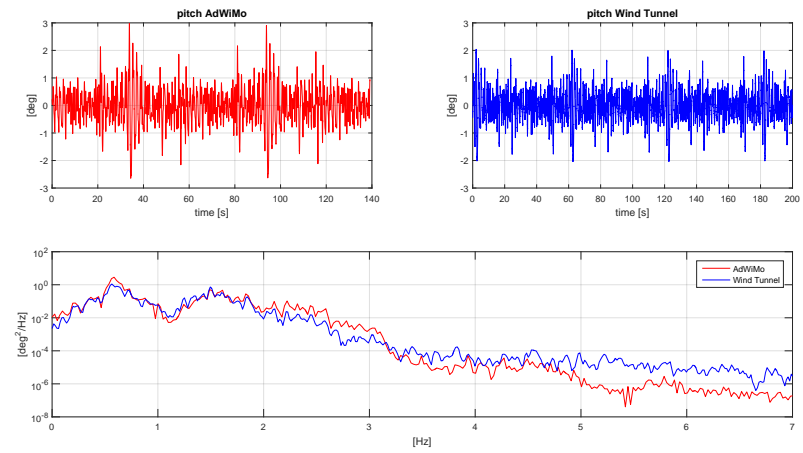


Figure 5.18: Pitch result for the irregular wave test in rated wind condition

Chapter 6

Conclusions and future developments

During this thesis work a complete integrated numerical model based on Adams/AdWiMo/Simulink co-simulation environment has been developed to account for the complete dynamic system (hexapod robot, wind turbine, rotor control, HIL algorithm) that will be tested in the Polimi wind tunnel. At first the model has been validated in a series of imposed sinusoidal surge motion tests, in order to understand if AdWiMo was able to reproduce correctly the Polimi wind turbine. The results of this first test campaign have shown an excellent agreement in terms of thrust force mean value, while they have indicated some differences in terms of amplitude variation, but those errors were anticipated from the previous simulations made in FAST environment during the development of the LIFES50+ project.

Then the model has been validated against a reduced order experimental setup (2 DoF), with regard to the aerodynamic forces computed in the numeric environment as well as the HIL methodology effectively implemented for various conditions (free decay in still water and air, regular and irregular sea state with wind).

The decay tests, made in absence of wind, have shown a perfect comparison with the real response of the system obtained in the wind tunnel, indicating that the inertial correction method for the calculation of the aerodynamic forces has been correctly modeled in the numerical rig.

The validation, made for different sea state, has shown a promising extension to a more complex but more complete 6 DoF model, making this tool valuable of the numerical benchmark and the design of experiments in that it allows to assess directly the control strategies of the wind turbine, of the

robot and of the HIL algorithm, which are effectively deployed onto the real-time hardware.

At this point the validated numerical tool is being used for assessing the correctness of the overall methodology on the 6-DoF system as well as specific load cases in the late stages of the robot constructions, to drive decisions at component level (i.e. custom-made joints dimensioning). Moreover, in order to make the developed tool even more reliable, a particular attention will be made to reproduce the closest simulations accounting also for the effective data exchange rates among the various modulus (e.g. sampling frequencies) reflecting the effective hardware performance [3].

Appendix A

Creation of the model in AdWiMo environment

In this appendix each step made, in the AdWiMo environment, for the creation of the wind turbine model, the addition of the hexapod robot, and the export of the system in the Simulink environment will be presented. This appendix can be seen as a sort of guide for AdWiMo, with a focus on the studied system.

Working area and database

This passage is not necessary but it is useful for a good and easy job setting. AdWiMo in fact needs some files as inputs for the structural and aerodynamic creation of the model, and furthermore it creates many output files for each modeling step and each analysis made. So it is recommended for the user to create a proper working area in which collect all the files needed for the work.

First of all, the base folder is created containing:

- a copy of the AdWiMo software, paying attention on modify inside its link properties the destination in which save the output files, in this way:

Da:

`%HOMEDRIVE%%HOMEPATH%%cwd%`

- a subfolder containing the five input files for the structural creation of the turbine (.tbb for the tower, .bbb for the blades, .hsp for the hub, .mgp for the generator and .gsp for the overall properties of the model)
- a subfolder containing the four macros provided by the MSC Software needed for the creation of a scaled wind turbine.

Now that the working area is complete, it is necessary to set the database of the AdWiMo coincident with the folder just created. In the software interface the user has to create the database selecting:

AdWiMo->Database Management->Create Database

and then complete the following window (figure A.1) with the desired name of the database and the path of the working folder. Finally the wanted

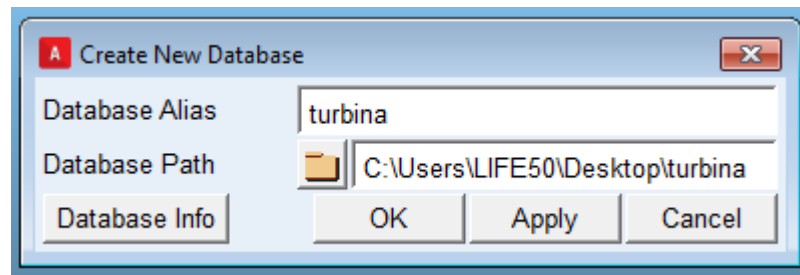


Figure A.1: "Create new Database" window

database has to be set as the working one:

AdWiMo->Database Management->Set Default Writable

AdWiMo, in addition, creates another folder in the working area, with the same name of the database, in which there are several subfolder, one for each topic of the aero-elasto analysis (e.g. flexible bodies, aerodynamic forces, wind, ...).

The last step consists in reading the necessary macros for working with scaled turbine. Selecting:

Tools->Macro->Read

the following window (figure A.2) will be opened:

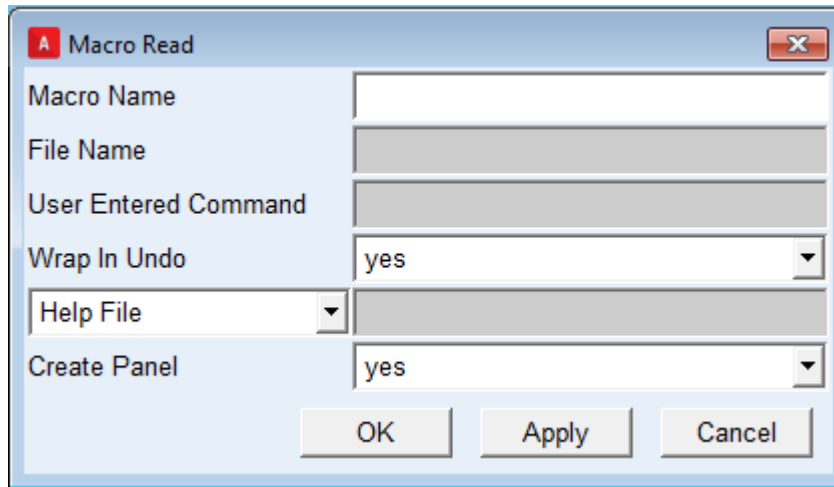


Figure A.2: "Macro Read" window

and it has to be completed in this way: in "Macro Name" the desired name of the macro and in "File Name" the path of the macro to be read. Then the user has to insert the name of the macro in the "Command Window" of AdWiMo.

Pre-process

This step is necessary in order to create all the binary files .mnf with which AdWiMo creates the structural model of the wind turbine. In order to do that the software reads the five input files collected in the subfolder in the working area, and then with Nastran creates the binary ones.

The logic under each input file is explained more in detail in Chapter 3. Every .mnf files is automatically saved in the database folder.

The five files are read by AdWiMo, as shown in the figure A.3, in this way:

```

AdWiMo->Preprocess Turbine->Preprocess Tower
AdWiMo->Preprocess Turbine->Preprocess Blade
AdWiMo->Preprocess Turbine->Preprocess Hub and Mainshaft
AdWiMo->Preprocess Turbine->Preprocess Main- and Generatorframe
AdWiMo->Preprocess Turbine->Create Turbine Property File

```

where in the last passage, the one regarding the general properties of the wind turbine, the file .gsp has to be modified by entering the paths of the .mnf files created by AdWiMo with the previous four passages.

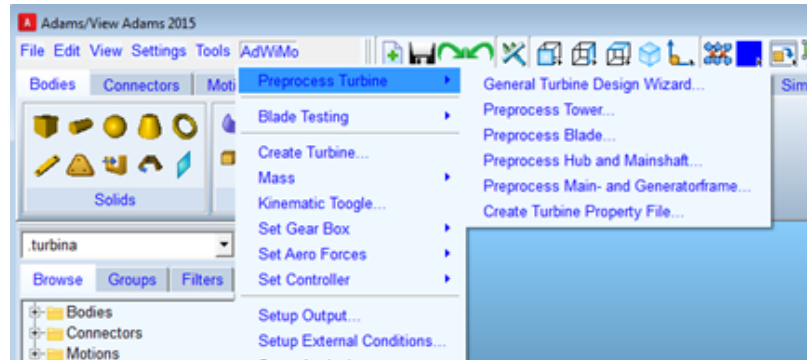


Figure A.3: Pre-process commands

Creation of the turbine, aerodynamic forces and rotor control

AdWiMo is now ready to construct the scaled wind turbine. Using the command:

AdWiMo->Create Turbine

and inserting the path of the .gsp file in the first row of the following window (the other paths are automatically found and inserted by the software): Once that the structural part of the model is completed, the user has to

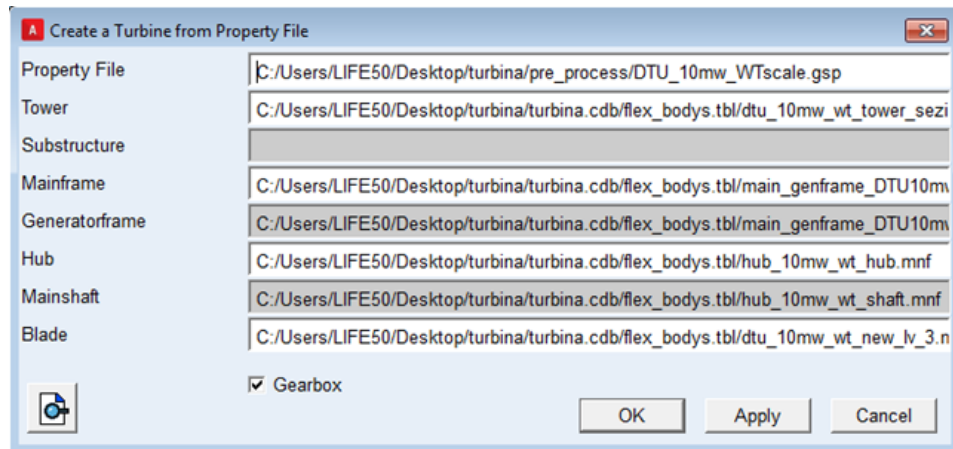


Figure A.4: "Create a new turbine" window

introduce the aerodynamic forces acting on the blades (AdWiMo gives the possibility to add them also on the tower and on the nacelle). First of all, it

is necessary to place the input file .ipt for the aerodynamic loads, equals to the one needed in FAST environment, in the database folder, with the file .wnd that describes the time history of the wind.

Then with the command:

AdWiMo->Set Aero Forces->Blade

a set of forces and torques are placed along each blade by simply insert the path of the .ipt file in the related window (figure A.5).

The modulus of the loads is function of the wind characteristics, so they

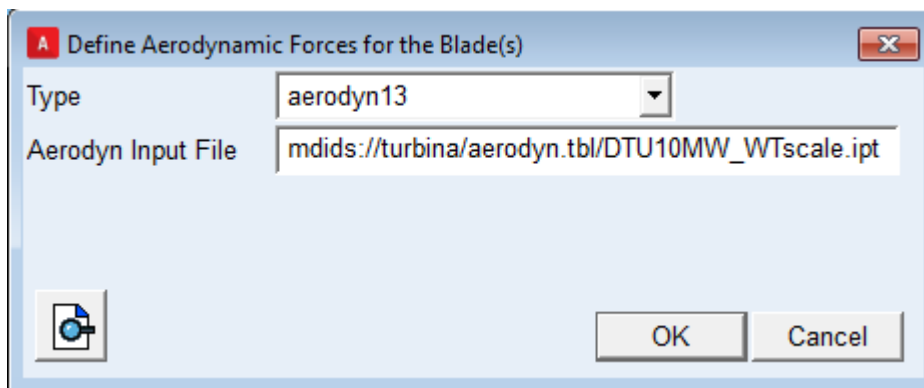


Figure A.5: Aerodynamic forces window

will be completely defined when the user will start a simulation (selecting the proper wind file).

The control of the rotor speed, as said in Chapter 3, can be made in two different ways: a constant motion, defined in velocity, placed between the rotor and the stator with the normal Adams command (see the figure A.6), or as a rotor control in with the use of the specific AdWiMo option.

In the second case, the user has to select:

AdWiMo->Set Controller->Generator Controller

and complete the following window (figure A.7) with the control type and the function describing the control logic.

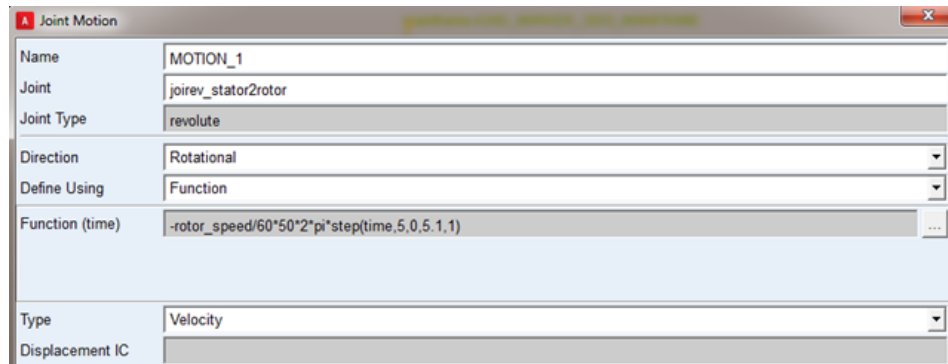


Figure A.6: Definition of the imposed rotor motion

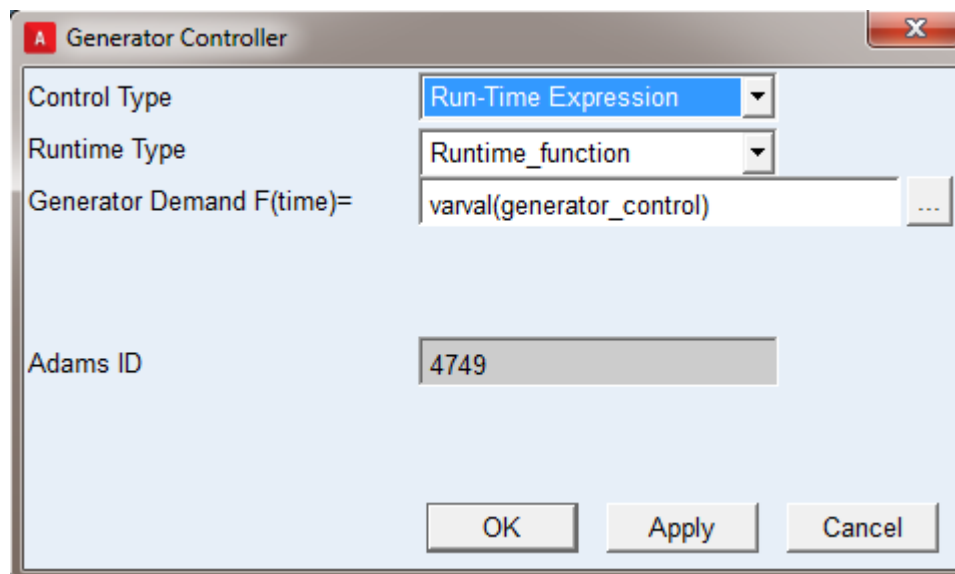


Figure A.7: "Generator Controller" window

Hexapod robot

The Adams model of the hexapod robot is made with a macro, that has been explained in the Chapter 3. It has been modified, for this application, to allow its assembly to the scaled wind turbine in the AdWiMo environment. The user has to simply add the macro to the software with the same method that has been used for the previous four macros, and AdWiMo will automatically construct the robot and constrain it to the turbine.

Exporting the model in Simulink environment

Adams provides a useful tool, named "Adams Control", that allows the user to export all the model in Simulink environment. Indicating the desired inputs and outputs, the tool creates a Simulink block that works like the AdWiMo model but independently from it.

The plug-in can be opened using the command:

Plugins->Control->Plant Export

that will open the following window (figure A.8).

After selecting Matlab as the target software, the user has to define the name of the model to export in the first two row, and then has to choose the inputs and the outputs of the block.

It is important to know that the inputs have to be defined as "State Variable" in AdWiMo, and their value has to be zero, because they will be overwritten every time step in the Simulink simulation.

The outputs, instead, have to be defined always as "State Variable", but their value has to be described as a measure of the wanted quantity.

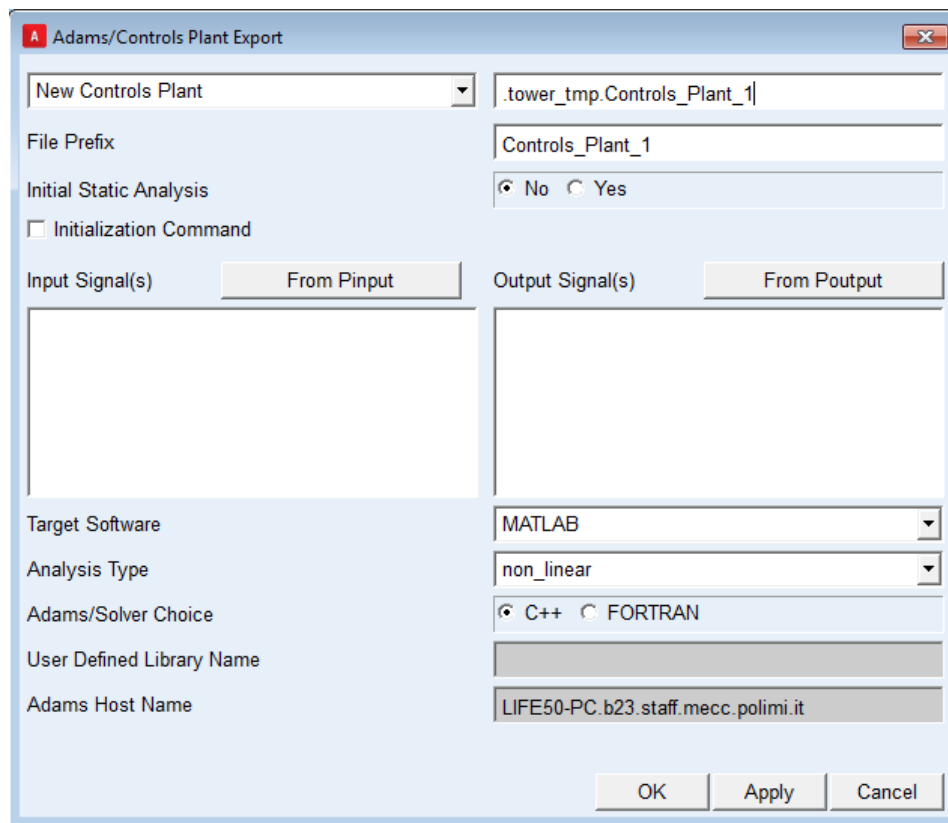


Figure A.8: "Adams Control" window

Appendix B

Implementation issues

In this appendix all the main issues encountered during the creation of the numerical model, and the relative solutions, are presented in form of a table.

Issues	Solutions
Creation of a scaled turbine model in AdWiMo environment	Utilization of the macros provided by MSC Software
Error on the mass properties (figure B.1) of the dummy bodies and singular inertial matrices	Creation of the 5 MW full scale turbine (AdWiMo reference) in order to use the needed mass parameters, properly upscaled and downscaled, in the Polimi turbine model
Presence of an "open" constraint in the nacelle zone	Manual modification of the position of the two markers related to this fixed joint
Need of a constant rotor speed	Two solutions: an imposed motion, defined in velocity, between stator and rotor or a rotor control torque. For the latter the two gain of the PI control are obtained from the rotor control made for the 5 MW full scale turbine, properly upscaled and downscaled

Tower vibration modes different from the expected ones	Modification of the .tbb input file for the tower, it contains only geometrical parameters, so they cannot be simply downscaled from the full scale tower, but they are obtained with the solution of the system of equations 3.1 presented in Chapter 3
Parameterization of the turbine markers in the macro used for the creation of the robot	All the bodies created by AdWiMo have to be parameterized with respect to the marker "origo", and no one else, for a software convention.
Imposed motion at the robot sliders in AdWiMo environment	Definition of the motion through an inverse kinematic approach made in Matlab environment, each slider motion has to be defined in velocity, in order to ensure the continuity of the splines up to the accelerations (and the the inertial forces)
Co-simulation in Simulink environment	<p>It is necessary that the AdWimo solver and the Simulink one have the same integration time step</p> <p>The type of the AdWiMo dynamic solver has been chosen with a "trial and error" method, a set of simple imposed motion simulations was carried out in order to check the correctness of the results</p> <p>The reaction forces at the tower base, essential for the inertial correction method, are extremely bad if the rotor speed is obtained with the imposed motion, so the implementation of the PI rotor control is necessary.</p>

Hydrodynamical model and correction of the inertial forces	The reaction forces at the base of the tower are measured respect to a rotating marker placed in the fixed joint that connects the robot platform and the tower
	Mass and inertial parameters of the wind turbine are obtained with the Adams command "Aggregate Mass", the momentum of inertia is properly modified using the formula 5.14
	The center of mass of the wind turbine is not perfectly aligned with the rotating marker introducing some errors in the measure of the reaction forces, this errors are eliminated though a Matlab function that is inserted in the Simulink model
	The filters that are present in the experimental setup introduce an error in the correction of the inertial forces, so they are not included in the numerical model
	The delays related to the actuation system present in the experimental setup are substituted with the integration step of the simulation

Table B.1: Issues encountered during the creation of the numerical model

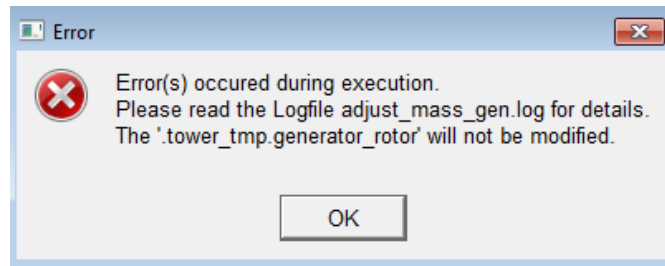


Figure B.1: Error on mass properties

Appendix C

Input file for the tower

```
$-----MDI_HEADER
[MDI_HEADER]
FILE_TYPE      = 'tbb'
FILE_VERSION   = 2.0
FILE_FORMAT    = 'ASCII'
CREATION_DATE  = '04 May 2017  16:09'
HEADER_SIZE    = 6
$-----UNITS
[UNITS]
LENGTH  = 'meter'
ANGLE   = 'degrees'
FORCE   = 'newton'
MASS    = 'kg'
TIME    = 'second'
$-----GENERAL
[GENERAL]
NUMBER_OF_PARTS      = 1
NUM_ELEMENTS_HEIGHT = 60
NUM_ELEMENTS_PERIMETER = 30
NUM_AEROFORCES      = 0
DRAG_COEFF          = 1.2
NUM_FIX_BOUND_NORMAL_MODES = 5
STRESS_OUTPUT       = 0
CRS_OUTPUT          = 0
```

\$-----FE_DATA

[FE_DATA]

YOUNGS_MODULUS = 2.10E+11
POISSONS_RATIO = 0.3
MATERIAL_DENSITY = 8500.0

\$-----SHAPE

[SHAPE]

{Section	Z_Coor.	Outer_Dia.	Point_Mass}
1	0.00000E+000	3.82000E-002	0.00000E+000
2	1.53000E-001	3.70000E-002	0.00000E+000
3	3.07000E-001	3.57000E-002	0.00000E+000
4	4.60000E-001	3.44000E-002	0.00000E+000
5	6.13000E-001	3.31000E-002	0.00000E+000
6	7.67000E-001	3.17000E-002	0.00000E+000
7	9.20000E-001	3.04000E-002	0.00000E+000
8	1.07300E+000	2.91000E-002	0.00000E+000
9	1.22700E+000	2.78000E-002	0.00000E+000
10	1.38000E+000	2.65000E-002	0.00000E+000
11	1.54200E+000	2.51000E-002	0.00000E+000

\$-----SECTION

[SECTION]

{Section	Wall_Thick.	Non_Struc_Mass}
1	1.50000E-003	0.00000E+000
2	1.40000E-003	0.00000E+000
3	1.40000E-003	0.00000E+000
4	1.30000E-003	0.00000E+000
5	1.20000E-003	0.00000E+000
6	1.10000E-003	0.00000E+000
7	1.00000E-003	0.00000E+000
8	1.00000E-003	0.00000E+000
9	9.00000E-004	0.00000E+000
10	8.00000E-004	0.00000E+000

Appendix D

Input file for the blades

```
$-----MDI_HEADER
[MDI_HEADER]
FILE_TYPE      = 'bbb'
FILE_VERSION   = 2.0
FILE_FORMAT    = 'ASCII'
CREATION_DATE  = '23 Oct 2015'
HEADER_SIZE    = 4

$-----UNITS
[UNITS]
LENGTH = 'meter'
ANGLE  = 'degrees'
FORCE  = 'newton'
MASS   = 'kg'
TIME   = 'second'

$-----FE_DATA
[FE_DATA]
YOUNGS_MODULUS      = 6.90E+10
POISSONS_RATIO      = 0.3
MATERIAL_DENSITY    = 2700.0

$-----GENERAL
[GENERAL]
```

```
NUMBER_OF_PARTS      = 1
NUMBER_OF_MODES      = 5
NUMBER_AERO_POINTS   = 39
ASPECT_RATIO_AERO    = 0.278
FLAG_RESVEC          = 1
FLAG_I_FACE_END      = 0
I_FAC_FLAP           = 1
I_FAC_EDGE            = 1
I_FAC_TORSION        = 1
CRS_OUTPUT           = 1
```

```
$-----BLADE_GEOMETRY
```

```
[BLADE_GEOMETRY]
```

```
{NUM  BLADE_LENGTH CHORD_LENGTH REL.THICKNESS
```

```
1.000000 0.000000 0.066090      1.000000
2.000000 0.044385 0.066090      1.000000
3.000000 0.088655 0.066090      0.873986
4.000000 0.133040 0.071049      0.359742
5.000000 0.177310 0.087777      0.180544
6.000000 0.221695 0.109003      0.132119
7.000000 0.266080 0.127877      0.105708
8.000000 0.310350 0.135934      0.100000
9.000000 0.354735 0.132326      0.100000
10.000000 0.399120 0.112373      0.100000
11.000000 0.443390 0.094259      0.100000
12.000000 0.487775 0.085109      0.100000
13.000000 0.532045 0.079955      0.100000
14.000000 0.576430 0.076031      0.100000
15.000000 0.620815 0.072519      0.100000
16.000000 0.665085 0.069112      0.100000
17.000000 0.709470 0.065594      0.100000
18.000000 0.753740 0.061956      0.100000
19.000000 0.798125 0.058361      0.100000
20.000000 0.842510 0.054958      0.100000
21.000000 0.886780 0.051615      0.100000
22.000000 0.931165 0.048163      0.100000
23.000000 0.975550 0.044859      0.100000
24.000000 1.019820 0.041606      0.100000
```

```
25.000000 1.064205 0.037953 0.100000
26.000000 1.108475 0.033556 0.100000
27.000000 1.152860 0.026716 0.100000
```

```
REL.POSITION AIRFOIL_ORIEN X_CROSS_REF. Y_CROSS_REF.}
```

```
0.500000 15.746980 0.000000 0.000000
0.500000 15.746980 0.000000 0.000000
0.500756 15.746980 0.000000 0.000000
0.462148 15.652752 0.000000 0.000000
0.383387 14.839226 0.000000 0.000000
0.323227 13.024817 0.000000 0.000000
0.293201 10.901871 0.000000 0.000000
0.290525 9.440541 0.000000 0.000000
0.290001 8.477581 0.000000 0.000000
0.290001 7.557063 0.000000 0.000000
0.290001 6.784215 0.000000 0.000000
0.290001 6.043631 0.000000 0.000000
0.290001 5.247443 0.000000 0.000000
0.290001 4.516308 0.000000 0.000000
0.290001 3.789474 0.000000 0.000000
0.290001 3.064021 0.000000 0.000000
0.290001 2.342582 0.000000 0.000000
0.290001 1.655435 0.000000 0.000000
0.290001 1.009227 0.000000 0.000000
0.290001 0.412286 0.000000 0.000000
0.290001 -0.143995 0.000000 0.000000
0.290001 -0.647529 0.000000 0.000000
0.290001 -1.117494 0.000000 0.000000
0.290001 -1.577579 0.000000 0.000000
0.290001 -2.027086 0.000000 0.000000
0.290001 -2.479742 0.000000 0.000000
0.290001 -2.881936 0.000000 0.000000
```

```
$-----BLADE_MASS
```

```
[BLADE_MASS]
```

```
{NUM BLADE_LENGTH MASS POLAR_MOMENT
```

```
1.000000 0.000000 0.230797 0.000242
```

```
2.000000 0.044385 0.230797 0.000244
```

3.000000	0.088655	0.230517	0.000218
4.000000	0.133040	0.202706	0.000167
5.000000	0.177310	0.219381	0.000121
6.000000	0.221695	0.264117	0.000096
7.000000	0.266080	0.300045	0.000080
8.000000	0.310350	0.309400	0.000067
9.000000	0.354735	0.305904	0.000057
10.000000	0.399120	0.299062	0.000050
11.000000	0.443390	0.289617	0.000041
12.000000	0.487775	0.277024	0.000034
13.000000	0.532045	0.263267	0.000028
14.000000	0.576430	0.248629	0.000023
15.000000	0.620815	0.233481	0.000017
16.000000	0.665085	0.218068	0.000014
17.000000	0.709470	0.202724	0.000010
18.000000	0.753740	0.187661	0.000008
19.000000	0.798125	0.172914	0.000005
20.000000	0.842510	0.158564	0.000005
21.000000	0.886780	0.144718	0.000003
22.000000	0.931165	0.131423	0.000002
23.000000	0.975550	0.118808	0.000002
24.000000	1.019820	0.107206	0.000001
25.000000	1.064205	0.095380	0.000001
26.000000	1.108475	0.079577	0.000000
27.000000	1.152860	0.001338	0.000000

ANGLE_INERTIA FLAP_I-MOMENT EDGE_I-MOMENT}

0.000000	0.000125	0.000117
0.000000	0.000126	0.000118
0.000000	0.000111	0.000107
39.423994	0.000077	0.000090
21.853310	0.000048	0.000073
12.406281	0.000031	0.000065
8.427325	0.000022	0.000058
6.630905	0.000017	0.000050
4.815239	0.000012	0.000046
4.237028	0.000010	0.000040
3.925467	0.000008	0.000034

3.369887 0.000006 0.000028
2.907994 0.000005 0.000023
2.445598 0.000003 0.000019
2.097964 0.000003 0.000015
1.743456 0.000002 0.000012
1.481770 0.000001 0.000009
1.238171 0.000001 0.000006
1.053807 0.000001 0.000005
0.900781 0.000001 0.000004
0.768666 0.000001 0.000003
0.666709 0.000000 0.000002
0.595553 0.000000 0.000001
0.539305 0.000000 0.000001
0.547129 0.000000 0.000001
0.675933 0.000000 0.000000
0.970123 0.000000 0.000000

\$-----BLADE_STIFFNESS

[BLADE_STIFFNESS]

{NUM BLADE_LENGTH ANGLE_PRIN.ST FW_BEND-STIFF

1.000000 0.000000 0.000000 1515.781282
2.000000 0.044385 0.000000 1515.781282
3.000000 0.088655 0.000000 1506.991091
4.000000 0.133040 39.423994 522.5891021
5.000000 0.177310 21.853310 153.1601988
6.000000 0.221695 12.406281 122.3610615
7.000000 0.266080 8.427325 114.4183415
8.000000 0.310350 6.630905 99.34052388
9.000000 0.354735 4.815239 91.94089225
10.000000 0.399120 4.237028 85.91041579
11.000000 0.443390 3.925467 78.02624981
12.000000 0.487775 3.369887 68.2867548
13.000000 0.532045 2.907994 58.61117733
14.000000 0.576430 2.445598 49.36892093
15.000000 0.620815 2.097964 40.88304364
16.000000 0.665085 1.743456 33.30757565
17.000000 0.709470 1.481770 26.76409133
18.000000 0.753740 1.238171 21.22774817


```

$-----BLADE_AXIS
[BLADE_AXIS]
{NUM BLADE_LENGTH X-AERO      Y-AERO
1.000000 0.000000 0.000000 0.000000
2.000000 0.044385 0.000000 0.000000
3.000000 0.088655 0.000000 0.000000
4.000000 0.133040 0.000000 0.000000
5.000000 0.177310 0.000000 0.000000
6.000000 0.221695 0.000000 0.000000
7.000000 0.266080 0.000000 0.000000
8.000000 0.310350 0.000000 0.000000
9.000000 0.354735 0.000000 0.000000
10.000000 0.399120 0.000000 0.000000
11.000000 0.443390 0.000000 0.000000
12.000000 0.487775 0.000000 0.000000
13.000000 0.532045 0.000000 0.000000
14.000000 0.576430 0.000000 0.000000
15.000000 0.620815 0.000000 0.000000
16.000000 0.665085 0.000000 0.000000
17.000000 0.709470 0.000000 0.000000
18.000000 0.753740 0.000000 0.000000
19.000000 0.798125 0.000000 0.000000
20.000000 0.842510 0.000000 0.000000
21.000000 0.886780 0.000000 0.000000
22.000000 0.931165 0.000000 0.000000
23.000000 0.975550 0.000000 0.000000
24.000000 1.019820 0.000000 0.000000
25.000000 1.064205 0.000000 0.000000
26.000000 1.108475 0.000000 0.000000
27.000000 1.152860 0.000000 0.000000

X-POS_SHEAR_C Y-POS_SHEAR_C X-POS_CoG
-0.000039      -0.000127      -0.000056
-0.000031      -0.000119      -0.000135
0.000325       0.000117       -0.000105
0.002834       0.000737       0.000865
0.008470       0.001272       0.002760
0.013824       0.001324       0.004754

```

0.014744	0.001631	0.005880
0.016676	0.001557	0.007335
0.017515	0.001283	0.007676
0.017615	0.000953	0.008094
0.017296	0.000789	0.008359
0.016673	0.000771	0.008291
0.015908	0.000791	0.008014
0.015106	0.000813	0.007567
0.014250	0.000828	0.007449
0.013378	0.000828	0.007144
0.012473	0.000804	0.006824
0.011596	0.000774	0.006541
0.010688	0.000718	0.006071
0.009816	0.000657	0.005574
0.008961	0.000602	0.005016
0.008177	0.000542	0.004583
0.007376	0.000489	0.004009
0.006629	0.000430	0.003304
0.005755	0.000380	0.002535
0.004643	0.000303	0.001424
0.002308	0.000153	0.000171

Y-POS_CoG X-POS_NEUTRAL Y-POS_NEUTRAL}

-0.000047	-0.000065	-0.000043
-0.000072	-0.000081	-0.000053
-0.000100	0.000030	-0.000067
0.000011	0.001290	0.000083
0.000233	0.003457	0.000181
0.000416	0.005827	0.000296
0.000525	0.007618	0.000405
0.000560	0.009516	0.000471
0.000481	0.009806	0.000400
0.000306	0.010315	0.000218
0.000233	0.010796	0.000141
0.000246	0.010603	0.000158
0.000285	0.010264	0.000197
0.000330	0.009826	0.000248
0.000361	0.009517	0.000284

0.000379	0.009009	0.000311
0.000381	0.008552	0.000320
0.000369	0.008030	0.000315
0.000350	0.007441	0.000300
0.000324	0.006826	0.000279
0.000298	0.006158	0.000256
0.000273	0.005560	0.000234
0.000254	0.004893	0.000218
0.000239	0.004170	0.000205
0.000227	0.003259	0.000199
0.000207	0.001941	0.000185
0.000125	0.000232	0.000117

Appendix E

Output file for the aerodynamic forces calculated by AeroDyn

This file was generated by AeroDyn
(v13.00.00a-bjj, 31-Mar-2010) on 23-Mar-2017.

Inputs read in from the AeroDyn input file:
Combined Experiment Baseline for AeroDyn version 12.5

SI Units for input and output
STEADY Dynamic stall model [NO Dynamic stall]
NO_CM Aerodynamic pitching moment model [NO Pitching Moments]
DYNIN Inflow model [Dynamic Inflow]
SWIRL Induction factor model [Normal and Radial flow
induction factors calculated]
5.00000E-03 Convergence tolerance for induction factor
[Not Used] Tip-loss model
[Not Used] Hub-loss model
"Wind_input.wnd" Wind file name
1.6 Wind reference (hub) height, m
0 Tower shadow centerline velocity deficit
1 Tower shadow half width, m
0 Tower shadow reference point, m

1.225 Air density, kg/m³
1.45000E-05 Kinematic air viscosity, m²/sec
1.00000E-03 Time interval for aerodynamic calculations, sec
39 Number of airfoil files used. Files listed below:
"airfoil.tbl/airfoileL_1_v2_Beddoes.dat"
"airfoil.tbl/airfoileL_2_v2_Beddoes.dat"
"airfoil.tbl/airfoileL_3_v2_Beddoes.dat"
"airfoil.tbl/airfoileL_4_v2_Beddoes.dat"
"airfoil.tbl/airfoileL_5_v2_Beddoes.dat"
"airfoil.tbl/airfoileL_6_v2_Beddoes.dat"
"airfoil.tbl/airfoileL_7_v2_Beddoes.dat"
"airfoil.tbl/airfoileL_8_v2_Beddoes.dat"
"airfoil.tbl/airfoileL_9_v2_Beddoes.dat"
"airfoil.tbl/airfoileL_10_v2_Beddoes.dat"
"airfoil.tbl/airfoileL_11_v2_Beddoes.dat"
"airfoil.tbl/airfoileL_12_v2_Beddoes.dat"
"airfoil.tbl/airfoileL_13_v2_Beddoes.dat"
"airfoil.tbl/airfoileL_14_v2_Beddoes.dat"
"airfoil.tbl/airfoileL_15_v2_Beddoes.dat"
"airfoil.tbl/airfoileL_16_v2_Beddoes.dat"
"airfoil.tbl/airfoileL_17_v2_Beddoes.dat"
"airfoil.tbl/airfoileL_18_v2_Beddoes.dat"
"airfoil.tbl/airfoileL_19_v2_Beddoes.dat"
"airfoil.tbl/airfoileL_20_v2_Beddoes.dat"
"airfoil.tbl/airfoileL_21_v2_Beddoes.dat"
"airfoil.tbl/airfoileL_22_v2_Beddoes.dat"
"airfoil.tbl/airfoileL_23_v2_Beddoes.dat"
"airfoil.tbl/airfoileL_24_v2_Beddoes.dat"
"airfoil.tbl/airfoileL_25_v2_Beddoes.dat"
"airfoil.tbl/airfoileL_26_v2_Beddoes.dat"
"airfoil.tbl/airfoileL_27_v2_Beddoes.dat"
"airfoil.tbl/airfoileL_28_v2_Beddoes.dat"
"airfoil.tbl/airfoileL_29_v2_Beddoes.dat"
"airfoil.tbl/airfoileL_30_v2_Beddoes.dat"
"airfoil.tbl/airfoileL_31_v2_Beddoes.dat"
"airfoil.tbl/airfoileL_32_v2_Beddoes.dat"
"airfoil.tbl/airfoileL_33_v2_Beddoes.dat"
"airfoil.tbl/airfoileL_34_v2_Beddoes.dat"

"airfoil.tbl/airfoileL_35_v2_Beddoes.dat"
 "airfoil.tbl/airfoileL_36_v2_Beddoes.dat"
 "airfoil.tbl/airfoileL_37_v2_Beddoes.dat"
 "airfoil.tbl/airfoileL_38_v2_Beddoes.dat"
 "airfoil.tbl/airfoileL_39_v2_Beddoes.dat"
 39 Number of blade elements per blade

Element (-)	RELM (m)	Twist (deg)	DR (m)	Chord (m)
1	0.05541	15.74698	0.03620	0.06609
2	0.09127	15.74698	0.03550	0.06609
3	0.12834	15.67759	0.03860	0.07011
4	0.16649	15.12031	0.03770	0.08316
5	0.20561	13.77216	0.04060	0.10128
6	0.24557	11.83058	0.03930	0.11974
7	0.28619	10.12019	0.04190	0.13327
8	0.32732	9.03967	0.04040	0.13664
9	0.36879	8.19962	0.04260	0.12833
10	0.41041	7.33580	0.04070	0.10656
11	0.45201	6.64275	0.04250	0.09192
12	0.49341	5.94630	0.04030	0.08430
13	0.53443	5.20612	0.04180	0.07972
14	0.57488	4.54173	0.03910	0.07616
15	0.61463	3.89061	0.04040	0.07300
16	0.65351	3.25502	0.03740	0.07001
17	0.69138	2.63168	0.03840	0.06705
18	0.72814	2.04967	0.03520	0.06407
19	0.76367	1.50642	0.03590	0.06114
20	0.79789	1.01251	0.03250	0.05838
21	0.83073	0.56754	0.03310	0.05585
22	0.86213	0.15988	0.02970	0.05348
23	0.89206	-0.20676	0.03020	0.05121
24	0.92049	-0.53005	0.02670	0.04899
25	0.94743	-0.82287	0.02720	0.04692
26	0.97288	-1.08974	0.02370	0.04505
27	0.99685	-1.33769	0.02430	0.04336
28	1.01939	-1.57314	0.02080	0.04164

29	1.04051	-1.78884	0.02140	0.03994
30	1.06027	-1.98741	0.01810	0.03829
31	1.07871	-2.17423	0.01880	0.03667
32	1.09590	-2.35320	0.01560	0.03496
33	1.11188	-2.51339	0.01640	0.03315
34	1.12671	-2.65687	0.01330	0.03123
35	1.14047	-2.77672	0.01420	0.02913
36	1.15320	-2.88480	0.01120	0.02664
37	1.16497	-2.98315	0.01230	0.02354
38	1.17584	-3.06505	0.00940	0.01921
39	1.18586	-3.13434	0.01060	0.00049

NFoil (-)	Print? (Yes/No)	Tip-loss constant	Hub-loss constant
--------------	--------------------	----------------------	----------------------

1	Yes	30.74958	0.72831
2	Yes	18.07872	2.17043
3	Yes	12.42356	3.66120
4	Yes	9.23307	5.19540
5	Yes	7.19097	6.76861
6	Yes	5.77674	8.37560
7	Yes	4.74393	10.00914
8	Yes	3.95933	11.66318
9	Yes	3.34544	13.33090
10	Yes	2.85406	15.00465
11	Yes	2.45334	16.67760
12	Yes	2.12163	18.34250
13	Yes	1.84365	19.99212
14	Yes	1.60839	21.61882
15	Yes	1.40736	23.21736
16	Yes	1.23439	24.78092
17	Yes	1.08461	26.30387
18	Yes	0.95413	27.78217
19	Yes	0.83995	29.21101
20	Yes	0.73959	30.58717
21	Yes	0.65106	31.90783
22	Yes	0.57271	33.17058
23	Yes	0.50317	34.37422

24	Yes	0.44130	35.51753
25	Yes	0.38610	36.60093
26	Yes	0.33676	37.62440
27	Yes	0.29260	38.58835
28	Yes	0.25296	39.49480
29	Yes	0.21738	40.34414
30	Yes	0.18537	41.13879
31	Yes	0.15656	41.88035
32	Yes	0.13058	42.57166
33	Yes	0.10714	43.21428
34	Yes	0.08599	43.81068
35	Yes	0.06685	44.36404
36	Yes	0.04956	44.87597
37	Yes	0.03390	45.34930
38	Yes	0.01972	45.78644
39	Yes	0.00688	46.18940

Rotor radius = 1.190 m

Hub radius = 0.037 m

Number of blades = 3

Blade element aerodynamic time series data written to file.

Bibliography

- [1] Simone Ambrosini. “Modellazione e caratterizzazione metrologica di un setup di tipo "HIL" per test in galleria del vento: il sistema eolico galleggiante OC5/5MW-NREL”. Master Thesis. Politecnico di Milano, 2016.
- [2] Marco Belloli Enrico Fiore Hermes Giberti. “Un manipolatore per prove dinamiche in galleria del vento con hardware-in-the-loop: analisi elastodinamica”. In: *Analisi e Calcolo* (2015).
- [3] Alan Facchinetti Ilmas Bayati Marco Belloli. “A 6 DoF/HIL setup for wind tunnel hybrid tests on a 1/75 scale model of a 10 MW floating wind turbine”. In: *The Italian Association of Theoretical and Applied Mechanics* (2017).
- [4] Alan Facchinetti Ilmas Bayati Marco Belloli. “Wind tunnel 2-DoF hybrid/HIL tests on the OC5 floating offshore wind turbine”. In: *OMAE2017* (2017).
- [5] Hermes Giberti Ilmas Bayati Marco Belloli. “Design of a 6-DoF Robotic Platform for Wind Tunnel Tests of Floating Wind Turbines”. In: *Energy Procedia* (2014).
- [6] Luca Bernini Ilmas Bayati Marco Belloli. “Aerodynamic design methodology for wind tunnel tests of wind turbine rotors”. In: *Journal of Wind Engineering and Industrial Aerodynamics* (2017).
- [7] Luca Bernini Ilmas Bayati Marco Belloli. “Wind tunnel validation of AeroDyn within LIFES50+ project: imposed Surge and Pitch tests”. In: *IOP Science* (2016).
- [8] Luca Bernini Ilmas Bayati Marco Belloli. *Wind turbine scaled model*. Politecnico di Milano, 2016.
- [9] Marshall L. Buhl Jr. Jason M. Jonkman. *FAST User’s Guide*. NREL, Aug. 2005.

- [10] B.J. Jonkman J.M. Jonkman G.J. Hayman. *AeroDyn v15 User's Guide and Theory Manual*. NREL.
- [11] *LIFES50+: Innovative Floating Offshore Wind Energy*. URL: lifes50plus.eu.
- [12] Henrik Bredmose Michael Borg Mahmood Mirzaei. *Wind turbine models for the design*. DTU, 2015.
- [13] MSC Software. *MSC AdWiMo manual, Release 2012R1*. 2012.